bioRxiv preprint doi: https://doi.org/10.1101/2020.05.08.083899; this version posted May 9, 2020. The copyright holder for this preprint (which was not certified by peer review) is the author/funder, who has granted bioRxiv a license to display the preprint in perpetuity. It is made available under aCC-BY-ND 4.0 International license.

Differential Response of Digesta- and Mucosa-Associated Intestinal Microbiota to Dietary Black Soldier Fly (*Hermetia illucens*) Larvae Meal in Seawater Phase Atlantic Salmon (*Salmo salar*)

Yanxian Li[a#], Leonardo Bruni[b], Alexander Jaramillo-Torres[a], Karina Gajardo[a*], Trond M. Kortner[a], Åshild Krogdahl[a]

[a]Department of Paraclinical Sciences, Faculty of Veterinary Medicine, Norwegian University of Life Sciences, Oslo, Norway.

[b]Department of Agriculture, Food, Environment and Forestry, University of Florence, Firenze, Italy.

Running Head: Response of Salmon Gut Flora to Dietary Insect Meal

[#]Address correspondence to Yanxian Li, yanxian.li@nmbu.no

[*]Present address: Biomar AS, Havnegata 9, 7010 Trondheim, Norway

Yanxian Li and Leonardo Bruni contributed equally to this work. Author order was selected based on CRediT (Contributor Roles Taxonomy).

Word counts: Abstract, 191 words; text, 4919 words

bioRxiv preprint doi: https://doi.org/10.1101/2020.05.08.083899; this version posted May 9, 2020. The copyright holder for this preprint (which was not certified by peer review) is the author/funder, who has granted bioRxiv a license to display the preprint in perpetuity. It is made available under aCC-BY-ND 4.0 International license.

ABSTRACT

Intestinal digesta is commonly used for studying responses of microbiota to dietary shifts, yet evidence is accumulating that it represents an incomplete view of the intestinal microbiota. In a 16-week seawater feeding trial, Atlantic salmon (*Salmo salar*) were fed either a commercially-relevant reference diet or an insect meal diet containing ~15% black soldier fly larvae meal. The digesta- and mucosa-associated distal intestinal microbiota were profiled by 16S rRNA gene sequencing. Regardless of diet, we observed substantial differences between digesta- and mucosa-associated intestinal microbiota. Microbial richness and diversity were much higher in the digesta than the mucosa. The insect meal diet altered the distal intestinal microbiota resulting in higher microbial richness and diversity. The diet effect, however, depended on the sample origin. Digesta-associated intestinal microbiota showed more pronounced changes than the mucosa-associated microbiota. Lastly, multivariate association analyses identified two mucosa-enriched taxa, *Brevinema andersonii* and unclassified *Spirochaetaceae*, associated with the expression of genes related to immune responses and barrier function in the distal intestine, respectively. Overall, our data clearly indicate that responses in digesta- and mucosa-associated microbiota to dietary inclusion of insect meal differ, with the latter being more resilient to dietary changes.

bioRxiv preprint doi: https://doi.org/10.1101/2020.05.08.083899; this version posted May 9, 2020. The copyright holder for this preprint (which was not certified by peer review) is the author/funder, who has granted bioRxiv a license to display the preprint in perpetuity. It is made available under aCC-BY-ND 4.0 International license.

IMPORTANCE

While fecal samples provide a convenient, non-invasive way for profiling intestinal microbiota, heterogeneity in the microbial community assemblage between intestinal digesta and mucosa is well recognized. The present work provides insights into the differences between digesta- and mucosa-associated intestinal microbiota in Atlantic salmon and how they respond differently to dietary perturbations. Mucosa-associated intestinal microbiota seemed more resilient to variation in diet composition than digesta-associated intestinal microbiota. Most likely, not only the digesta associated microbiota, but also the mucosa-associated, play key roles in shaping the host metabolism. Therefore, our work emphasizes the necessity of profiling both digesta- and mucosa-associated intestinal microbiota to understand the impact of variation in diet composition on intestinal microbiota.

KEYWORDS: microbiota, gut biogeography, Atlantic salmon, diet, black soldier fly

bioRxiv preprint doi: https://doi.org/10.1101/2020.05.08.083899; this version posted May 9, 2020. The copyright holder for this preprint (which was not certified by peer review) is the author/funder, who has granted bioRxiv a license to display the preprint in perpetuity. It is made available under aCC-BY-ND 4.0 International license.

INTRODUCTION

The reduction in the sequencing costs and the advent of bioinformatics in the past decade have enabled in-depth taxonomic and functional profiling of microbial communities from diverse environments at an unprecedented scale. Recent advances in the microbiome studies have shed light on the role of intestinal microbiota in a wide spectrum of host physiological processes and development of diseases, such as helping digestion and absorption (1), modulating lipid metabolism and energy balance (2, 3), dialoguing with the central nervous system through the so-called microbiota-gut-brain axis (4) and being a risk factor or a therapeutic intervention of inflammatory bowel disease (5-8). Diet is one of the key factors in shaping the intestinal microbiota. While long-term dietary habits have a considerable effect on the structure and activity of host intestinal microbiota (9-11), short-term dietary change also alters the intestinal microbiota in a rapid and reproducible way (12). Different dietary components selectively promote or suppress the growth of certain microbial clades, which in turn could inflict important effects on the host health and disease resistance (13, 14).

Atlantic salmon (*Salmo salar*) is the most produced seawater fish species and one of the most economically important farmed fish worldwide (15). While Atlantic salmon are strictly carnivorous in the wild, farmed Atlantic salmon have experienced a substantial shift in the diet composition due to a limited supply of marine ingredients. Marine ingredients used for Norwegian farmed Atlantic salmon have gradually been replaced by plant sources, decreasing from ~90% in 1990 to ~25% in 2016 (16). Due to concerns on

bioRxiv preprint doi: https://doi.org/10.1101/2020.05.08.083899; this version posted May 9, 2020. The copyright holder for this preprint (which was not certified by peer review) is the author/funder, who has granted bioRxiv a license to display the preprint in perpetuity. It is made available under aCC-BY-ND 4.0 International license.

the economic, environmental and social sustainability of the current raw materials for Atlantic salmon farming (15), more sustainable alternative feed ingredients, such as insects (17) and yeasts (18), have been developed and used. The use of alternative feed ingredients may not only affect the nutrient utilization, fish growth, health, welfare and product quality, but also intestinal microbiota in Atlantic salmon (19-21). While studies in mammals and fish have revealed substantial differences between the digesta- and mucosa-associated intestinal microbiota (19, 22-25), most studies investigating diet effects on the intestinal microbiota of fish have sampled the digesta only or a mixture of digesta and mucosa. Evidence is accumulating that digesta- and mucosa-associated intestinal microbiota in fish respond differently to dietary changes (19, 26-29). Profiling only one of or a mixture of digesta- and mucosa-associated microbiota may obscure the response of intestinal microbiota to dietary changes.

Characterizing intestinal microbiota and its associations with host responses is an essential step towards identifying key microbial clades promoting fish health and welfare. Ultimately, a milestone in the fish microbiota research would be knowing how to selectively manipulate the microbiota to improve the growth performance, disease resistance and health status of farmed fish. The main aims of the work presented herein were (i) to compare distal intestinal microbiota of Atlantic salmon fed a commercially relevant diet and an insect meal-based diet, (ii) to further explore the dissimilarity between digesta- and mucosa-associated microbiota and the differences in their response to dietary changes, and (iii) to identify associations between microbial clades and host responses. This work was part of a larger study consisting of a freshwater and seawater

bioRxiv preprint doi: https://doi.org/10.1101/2020.05.08.083899; this version posted May 9, 2020. The copyright holder for this preprint (which was not certified by peer review) is the author/funder, who has granted bioRxiv a license to display the preprint in perpetuity. It is made available under aCC-BY-ND 4.0 International license.

feeding trial that aimed to investigate the nutritional value and possible health effects for Atlantic salmon of a protein-rich insect meal produced from black soldier fly (*Hermetia illucens*) larvae. The present work focuses on the intestinal microbiota in seawater-phase Atlantic salmon fed an insect meal diet containing ~15% black soldier fly larvae meal for 16 weeks. Results on feed utilization, growth performance, fillet quality, intestinal histomorphology and gene expression have been reported elsewhere (30-32).

RESULT

Hereafter, different sample groups are named based on the combination of diet (REF vs. IM) and sample origin (DID vs. DIM). Hence, in addition to the extraction blanks, library blanks and mock, we have four different sample types, i.e., REF-DID, REF-DIM, IM-DID and IM-DIM.

qPCR

Since Cq values of most mucosa DNA templates were out of the linear range of the standard curve, the raw Cq value was used as a proxy of 16S rRNA gene quantity in the diluted DNA templates (Figure S1). On average, REF-DID showed the highest 16S rRNA gene quantities (mean Cq = 24.7), followed by the mocks (mean Cq = 26.1) and IM-DID (mean Cq = 28.4). Irrespective of diet, mucosa DNA templates (REF-DIM, IM-DIM) showed similar 16S rRNA gene quantities (mean Cq = 30) that were close to extraction blanks (mean Cq = 32.4).

Taxonomic composition

All the eight bacterial species included in the mock were successfully identified at

bioRxiv preprint doi: https://doi.org/10.1101/2020.05.08.083899; this version posted May 9, 2020. The copyright holder for this preprint (which was not certified by peer review) is the author/funder, who has granted bioRxiv a license to display the preprint in perpetuity. It is made available under aCC-BY-ND 4.0 International license.

genus level with *E. faecalis, L. fermentum, L. monocytogenes* and *S. aureus* further being annotated at the species level (Figure S2A). At the genus level, the average Pearson's *r* between the expected and observed taxonomic profile of the mock was 0.33, whereas the Pearson's *r* between the observed taxonomic profile of the mock was 0.98. The relative abundance of most Gram-positive bacteria, *L. monocytogenes* and *E. faecalis* in particular, were underestimated. In contrast, the relative abundance of Gram-negative bacteria was overestimated. Most ASVs (97.5% - 99.9%) in the extraction and library blanks were classified as *Pseudomonas* (Figure S2B), which was the main contaminating taxon removed from the biological samples along with other contaminants including *Curtobacterium*, *Jeotgalicoccus*, *Modestobacter*, *Cutibacterium*, *Hymenobacter*, *Brevundimonas*, *Micrococcus*, *Sphingomonas*, *Devosia*, *Sphingomonas aurantiaca* and *Marinobacter adhaerens*. The exact sequence of the contaminating ASVs and their relative abundance in the extraction and library blanks are available in Table S1.

The taxonomic composition of mucosa samples showed higher similarity than that of the digesta samples, which were more diet-dependent (Figure 1). At the phylum level, the dominant taxa of mucosa samples for both diets were *Spirochaetes* (REF-DIM, 72 ± 34.6 %; IM-DIM, 47 ± 35.2 %) (mean ± S.D.), *Proteobacteria* (REF-DIM, 21 ± 34.1 %; IM-DIM, 23 ± 34.1 %), *Firmicutes* (REF-DIM, 1 ± 2.8 %; IM-DIM, 11 ± 13.5 %), *Tenericutes* (REF-DIM, 4 ± 8 %; IM-DIM, 8 ± 18.8 %) and *Actinobacteria* (REF-DIM, 1 ± 3.4 %; IM-DIM, 9 ± 8.7 %). For digesta samples, the dominant taxa of REF-DID were *Tenericutes* (33 ± 23.1 %), *Proteobacteria* (31 ± 29.9 %), *Firmicutes* (25 ± 21.1 %) and *Spirochaetes* (9 ± 12.9 %), whereas IM-DID was dominated by *Firmicutes* (45 ±

bioRxiv preprint doi: https://doi.org/10.1101/2020.05.08.083899; this version posted May 9, 2020. The copyright holder for this preprint (which was not certified by peer review) is the author/funder, who has granted bioRxiv a license to display the preprint in perpetuity. It is made available under aCC-BY-ND 4.0 International license.

16.9 %), *Actinobacteria* (25 ± 9.5 %), *Proteobacteria* (17 ± 27.8 %), *Tenericutes* (7 ± 8.8 %) and *RsaHF231* (4 ± 1.5 %) (Figure 1A). At the genus level, the dominant taxa of mucosa samples for both diets were *Brevinema* (REF-DIM, 52 ± 40.1 %; IM-DIM, 25 ± 35 %), unclassified *Spirochaetaceae* (REF-DIM, 20 ± 31.8 %; IM-DIM, 22 ± 31.4 %), *Aliivibrio* (REF-DIM, 18 ± 33.5 %; IM-DIM, 18 ± 35.3 %) and *Mycoplasma* (REF-DIM, 4 ± 8 %; IM-DIM, 8 ± 18.8 %). For digesta samples, the dominant taxa of REF-DID were *Mycoplasma* (33 ± 23.1 %), *Aliivibrio* (20 ± 32.3 %), *Photobacterium* (10 ± 12.6 %), *Brevinema* (6 ± 12.5 %) and *Lactobacillus* (5 ± 4 %), whereas IM-DID was dominated by *Aliivibrio* (15 ± 28.2 %), unclassified *Lactobacillales* (14 ± 6 %), *Corynebacterium 1* (13 ± 5 %), *Bacillus* (8 ± 3.4 %), *Mycoplasma* (7 ± 8.8 %) and *Actinomyces* (5 ± 2 %) (Figure 1B).

Core microbiota

In total, 108 taxa were identified as core microbiota based on their prevalence in each sample type (Figure 2; Table S2). Specifically, *Aliivibrio*, *Brevinema andersonii*, and *Mycoplasma* were identified as core microbiota for all the sample types, the latter two being universally present in all the samples. Additionally, ten taxa were identified as core microbiota for digesta samples (REF-DID and IM-DID), which included *Bacillus*, *Corynebacterium 1*, *Lactobacillus* (*L. aviaries, L. fermentum* and two unclassified species), *Leuconostoc*, *Parageobacillus toebii*, *Ureibacillus* and *Weissella*. No additional core microbiota taxa were identified for the mucosa samples (REF-DIM and IM-DIM). *Actinomyces*, *Corynebacterium 1*, *Corynebacterium aurimucosum* ATCC 70097, *Microbacterium* and unclassified *RsaHF23* were the additional core microbiota taxa

bioRxiv preprint doi: https://doi.org/10.1101/2020.05.08.083899; this version posted May 9, 2020. The copyright holder for this preprint (which was not certified by peer review) is the author/funder, who has granted bioRxiv a license to display the preprint in perpetuity. It is made available under aCC-BY-ND 4.0 International license.

identified for fish fed the insect meal diet (IM-DID and IM-DIM), whereas no additional core microbiota taxa were identified for fish fed the reference diet (REF-DID and REF-DIM). Lastly, 86 taxa were found to be more prevalent in IM-DID than in any other sample type.

Alpha-diversity

Regardless of diet, all the alpha-diversity indices were higher in digesta samples than mucosa samples ($p < 0.05$) (Figure 3). Independent of sample origin, all the alpha-diversity indices were higher in fish fed the IM diet than those fed the REF diet ($p < 0.05$). A significant interaction between the diet and sample origin effect was detected for the observed species ($p = 0.031$) and Faith's phylogenetic diversity ($p = 0.002$), both of which showed a stronger diet effect in digesta samples than mucosa samples.

Beta-diversity

The PCoA plots built on the Jaccard and unweighted UniFrac distance matrix showed clear separations of samples belonging to different dietary groups and sample origins (Figure 4A-B). However, the average distance between samples from different dietary groups was dependent on sample origin. Specifically, mucosa samples from different dietary groups formed clusters close to each other, whereas digesta samples from different dietary groups were far apart. The PCoA plots built on the Aitchison and PHILR transformed Euclidean distance matrix also showed separations of samples belonging to different dietary groups and sample origins (Figure 4C-D). Again, the average distance between samples from different dietary groups was dependent on sample origin. Mucosa samples from different dietary groups formed clusters boarding (Figure 4C) or

bioRxiv preprint doi: https://doi.org/10.1101/2020.05.08.083899; this version posted May 9, 2020. The copyright holder for this preprint (which was not certified by peer review) is the author/funder, who has granted bioRxiv a license to display the preprint in perpetuity. It is made available under aCC-BY-ND 4.0 International license.

overlapping (Figure 4D) each other, whereas digesta samples from different dietary groups were more clearly separated.

The PERMANOVA and its following conditional contrasts largely confirmed the PCoA results. Regardless of the distance matrix used, both main factors had significant effects on the beta-diversity and their interaction was significant as well ($p < 0.05$) (Table 1). Results on the tests of homogeneity of multivariate dispersions are shown in Table 2. For Jaccard distance, significant differences in the multivariate dispersions were observed between digesta and mucosa samples for both diets (REF-DID VS. REF-DIM, $p = 0.045$; IM-DID VS. IM-DIM, $p = 0.002$), and between diets for digesta samples (REF-DID VS. IM-DID, $p = 0.002$). For unweighted UniFrac distance, IM-DID showed lower multivariate dispersions than other sample types resulting in significant differences compared to REF-DID ($p = 0.002$) and IM-DIM ($p = 0.002$). For Aitchison distance, REF-DIM showed lower multivariate dispersions than other sample types resulting in significant differences compared to REF-DID ($p = 0.046$) and IM-DIM ($p = 0.046$). For PHILR transformed Euclidean distance, the differences in the multivariate dispersions among the sample types were not significant ($p > 0.05$).

Significant associations between microbial clades and sample metadata

The multivariate association analysis identified 53 taxa showing significant associations with the metadata of interest (Figure 5A). The diagnostic plots showing the raw data underlying the significant associations are shown in Figures S3-8. Forty-seven differentially abundant taxa were identified for the sample origin effect, 45 of which, including *Bacillus*, *Enterococcus*, *Flavobacterium*, *Lactobacillus*, *Lactococcus*,

bioRxiv preprint doi: https://doi.org/10.1101/2020.05.08.083899; this version posted May 9, 2020. The copyright holder for this preprint (which was not certified by peer review) is the author/funder, who has granted bioRxiv a license to display the preprint in perpetuity. It is made available under aCC-BY-ND 4.0 International license.

Leuconostoc, *Mycoplasma*, *Peptostreptococcus*, *Photobacterium*, *Staphylococcus*, *Streptococcus*, *Vagococcus* and *Weissella*, showed lower relative abundances in the mucosa than the digesta (Figure S3). In contrast, two taxa belonging to the *Spirochaetes* phylum, *B. andersonii* and unclassified *Spirochaetaceae*, were enriched in the mucosa (Figure 5B). Thirty-six differentially abundant taxa were identified for the diet effect, 26 of which showed increased relative abundances in fish fed the IM diet (Figure S4). Among these 26 taxa, some were enriched in both intestinal digesta and mucosa which included *Actinomyces*, unclassified *Bacillaceae*, *Bacillus*, unclassified *Beutenbergiaceae*, *Brevibacterium*, *Corynebacterium 1*, *Enterococcus*, unclassified *Lactobacillales*, *Microbacterium*, *Oceanobacillus* and unclassified *RsaHF231* (partially illustrated as Figure 5C). For the histological scores, the relative abundance of unclassified *Sphingobacteriaceae* and unclassified *RsaHF231* were found to increase and decrease, respectively, in fish scored abnormal regarding lamina propria cellularity (lpc) in distal intestine (Figure S5). The relative abundance of *Acinetobacter* and *Pseudomonas* were negatively correlated with the distal intestine somatic index (DISI) (Figure S6). Six taxa, including *Actinomyces*, *B. andersonii*, *Kurthia*, *Lysobacter*, *Microbacterium* and the unclassified *Sphingobacteriaceae*, were found to associate with the expression of genes related to immune responses (Figure S7). Notably, the relative abundance of *B. andersonii* showed a clear positive correlation with the expression levels of immune genes (Figure 5D), which decreased as the PC1 of the PCA increased. Furthermore, 3 taxa including *Cellulosimicrobium*, *Glutamicibacter* and the unclassified *Spirochaetaceae* were found to associate with the expression of genes related to barrier functions (Figure S8). The

bioRxiv preprint doi: https://doi.org/10.1101/2020.05.08.083899; this version posted May 9, 2020. The copyright holder for this preprint (which was not certified by peer review) is the author/funder, who has granted bioRxiv a license to display the preprint in perpetuity. It is made available under aCC-BY-ND 4.0 International license.

relative abundance of the unclassified *Spirochaetaceae* showed a negative correlation with the expression levels of barrier function relevant genes (Figure 5E), which decreased as the PC1 of the PCA increased.

DISCUSSION

Core microbiota

In accordance with previous studies in Atlantic salmon (20, 33-38), *Aliivibrio*, *B. andersonii* and *Mycoplasma* were identified as core microbiota in the present study. *Aliivibrio* is commonly found in the seawater phase Atlantic salmon intestine (35-37, 39-43) and has been identified as a core taxon of both wild and captive Atlantic salmon (34, 36, 37). Provided its common presence in seawater, *Aliivibrio* may have originated from the surrounding water and colonized the intestinal mucosa as Atlantic salmon constantly drink seawater to prevent dehydration in a hyperosmotic environment. Currently, the taxon *Aliivibrio* comprises of four closely related species including *Aliivibrio fischeri*, *Aliivibrio logei*, *Aliivibrio salmonicida* and *Aliivibrio wodanis*, which were split from the *Vibrio* genus and reclassified as *Aliivibrio* in 2007 (44). Strains of *A. fischeri* and *A. logei* have been described as bioluminescent symbionts of certain fishes and squids (45), whereas *A. salmonicida* and *A. wodanis* have been identified as pathogens for Atlantic salmon causing cold-water vibriosis (46) and 'winter ulcer' (47), respectively.

Though *Spirochaetes* has typically been found in low abundances in the Atlantic salmon intestine (19, 23, 27, 39), two recent studies have identified *B. andersonii* as a core taxon of both digesta- and mucosa-associated intestinal microbiota in seawater phase

bioRxiv preprint doi: https://doi.org/10.1101/2020.05.08.083899; this version posted May 9, 2020. The copyright holder for this preprint (which was not certified by peer review) is the author/funder, who has granted bioRxiv a license to display the preprint in perpetuity. It is made available under aCC-BY-ND 4.0 International license.

Atlantic salmon (35, 36). Furthermore, *B. andersonii* is also a predominant taxon in the digesta and mucosa in one of the studies (36). *B. andersonii* was initially isolated from short-tailed shrews (*Blarina brevicauda*) and white-footed mice (*Peromyscus leucopus*) as an infectious pathogen (48). This taxon has also been found in the intestine and gill tissue of rainbow trout (*Oncorhynchus mykiss*) (49), and intestinal digesta of Senegalese sole (*Solea senegalensis*)(50).

Mycoplasma is widely distributed in nature and well known for its minute size and lack of cell wall. Like *Aliivibrio*, *Mycoplasma* has been frequently identified as a core taxon of both wild and captive Atlantic salmon as well (20, 33, 35-38). It was found to be more abundant in marine adults than in freshwater juvenile Atlantic salmon (37) and sporadically predominate intestinal microbial community in the digesta (20, 36, 37, 41, 51) and mucosa (35) reaching as high as > 90% of total read counts in extreme cases. Due to its small compact genome and limited biosynthesis capacities, *Mycoplasma* typically forms obligate parasitic or commensal relationships with its host to obtain necessary nutrients such as amino acids, fatty acids and sterols (52). The major acids produced by *Mycoplasma* during fermentation are lactic acid and acetic acid (53), the latter of which was found in our recent studies to be 2-4 orders of magnitude higher than other short-chain fatty acids in the Atlantic salmon distal intestine (unpublished data). A recent study found that Atlantic salmon *Mycoplasma*, recovered by shotgun metagenomic sequencing, was closely related to *Mycoplasma penetrans* and *Mycoplasma yeatsii* (20). Compared to these closely related *Mycoplasma* species, the salmon *Mycoplasma* appears to carry a much lower number of unique genes that are enriched in carbohydrate uptake and low in

bioRxiv preprint doi: https://doi.org/10.1101/2020.05.08.083899; this version posted May 9, 2020. The copyright holder for this preprint (which was not certified by peer review) is the author/funder, who has granted bioRxiv a license to display the preprint in perpetuity. It is made available under aCC-BY-ND 4.0 International license.

peptidase synthesis.

Sample origin effect

In line with previous findings in mammals and fish (19, 22-25), we observed substantial differences between digesta- and mucosa-associated microbiota. The microbial richness and diversity were much higher in the digesta than the mucosa, as previously observed in seawater phase Atlantic salmon (19, 23, 36). Furthermore, most of the bacterial taxa in the distal intestine, including those commonly found in the Atlantic salmon intestine such as *Bacillus*, *Enterococcus*, *Flavobacterium*, *Lactobacillus*, *Lactococcus*, *Leuconostoc*, *Mycoplasma*, *Peptostreptococcus*, *Photobacterium*, *Staphylococcus*, *Streptococcus*, *Vagococcus* and *Weissella*, were less abundant in the mucosa than in the digesta. These results are suggestive of a selection pressure from the host that determines which microbial clades colonize and flourish in the intestinal mucus layer (54). In this study, two taxa belonging to the *Spirochaetes* phylum, *B. andersonii* and unclassified *Spirochaetaceae*, were more abundant in the distal intestine mucosa than the digesta. As aforementioned, *Spirochaetes* were typically found in low abundances in the Atlantic salmon intestine. Yet a recent study also showed that irrespective of diets *B. andersonii* seemed to be more abundant in the intestinal mucosa than the digesta of seawater phase Atlantic salmon (36). Known for high motility and chemotactic attraction to mucin, some *Spirochaetes* can penetrate the mucus and associate with the intestinal mucosa (55-57). Further work is required to confirm whether these taxa are consistently enriched in the intestinal mucus layer of seawater phase Atlantic salmon.

bioRxiv preprint doi: https://doi.org/10.1101/2020.05.08.083899; this version posted May 9, 2020. The copyright holder for this preprint (which was not certified by peer review) is the author/funder, who has granted bioRxiv a license to display the preprint in perpetuity. It is made available under aCC-BY-ND 4.0 International license.

Diet effect

Diet is one of the key factors in shaping the fish intestinal microbiota. In agreement with previous findings in rainbow trout (29, 58, 59) and laying hens (60, 61), we found that the insect meal diet altered the distal intestinal microbiota assemblage resulting in higher microbial richness and diversity. Our findings, showing that the insect meal diet increased the relative abundance of *Actinomyces, Bacillus, Brevibacterium, Corynebacterium 1 and Enterococcus,* are in accord with recent studies in rainbow trout fed diets containing 30% black soldier fly larvae meal (29, 59). Importantly, these results were partly confirmed in other studies employing fluorescence *in situ* hybridization for targeted profiling of changes in the intestinal microbiota. Specifically, increased absolute abundance of *Lactobacillus*/*Enterococcus* was found in rainbow trout fed 20% dietary black soldier fly larvae meal (62), whereas increased absolute abundance of *Bacillus*, *Enterococcus* and *Lactobacillus* was documented in Siberian sturgeon (*Acipenser baerii*) fed 15% black soldier fly larvae meal (63).

The increases in the relative abundance of specific microbial clades in Atlantic salmon fed the insect meal diet may be explained by feed-borne microbiota and/or feed composition. Bacterial taxa, including *Actinomyces*, *Bacillus*, *Brevibacterium*, *Corynebacterium*, *Enterococcus*, *Oceanobacillus* and *RsaHF231*, have been found in black soldier fly whole larvae or larvae intestine (64-67). The fact that *RsaHF231* has not been documented in fish before indicates that these bacterial taxa may have partially originated from black soldier fly larvae meal. Our results from the freshwater feeding trial showed that these bacterial taxa were also enriched in the intestinal digesta and mucosa

bioRxiv preprint doi: https://doi.org/10.1101/2020.05.08.083899; this version posted May 9, 2020. The copyright holder for this preprint (which was not certified by peer review) is the author/funder, who has granted bioRxiv a license to display the preprint in perpetuity. It is made available under aCC-BY-ND 4.0 International license.

of Atlantic salmon smolts fed an insect meal diet containing 60% soldier fly larvae meal. Importantly, these bacterial taxa were also detected in the feed pellets which contained considerable amount of bacterial DNA that is comparable to intestinal digesta (unpublished data). Given the hydrothermal treatments the feed pellets underwent during the extrusion, the feed-borne microbiota profiled by the DNA sequencing techniques could have largely originated from dead bacteria and bacterial spores rather than living bacteria. As sequencing-based methods cannot differentiate between living and dead cells, future studies should investigate to what extent the feed-borne microbiota may contribute to, or confound the observed diet effects on intestinal microbiota, using methods that distinguish living and dead bacteria such as viability PCR and RNA sequencing (68). On the other hand, unique nutrients in the insect meal diet such as chitin, an essential component of the insect exoskeleton, may have selectively promoted the growth of certain intestinal microbes. *Actinomyces* species are often identified as active chitin degraders showing enhanced growth and activity upon chitin addition (69). Many bacterial species belonging to *Bacillus* can produce chitinase (70). *Bacillus* and *Lactobacillus* were two of the predominant taxa in the intestinal mucosa of Atlantic salmon fed a 5% chitin diet, the former of which displayed the highest *in vitro* chitinase activity (71).

Significant interactions between diet and sample origin effect

We observed in the present study that the diet effect on the intestinal microbial community richness and structure was dependent on the sample origin, with mucosa-associated intestinal microbiota showing higher resilience to the dietary change. Our results corroborate previous findings in rainbow trout revealing that mucosa-associated

bioRxiv preprint doi: https://doi.org/10.1101/2020.05.08.083899; this version posted May 9, 2020. The copyright holder for this preprint (which was not certified by peer review) is the author/funder, who has granted bioRxiv a license to display the preprint in perpetuity. It is made available under aCC-BY-ND 4.0 International license.

intestinal microbiota was less influenced by dietary inclusion of 30% black soldier fly larvae meal compared to digesta-associated intestinal microbiota (28, 29). Results from molecular-based studies on salmonid intestinal microbiota hitherto suggest that diet modulates digesta- and mucosa-associated intestinal microbiota to varying degrees with the latter generally being more resilient to dietary interventions (19, 26-29, 35). As such, current practices of profiling only one of or a mixture of digesta- and mucosa-associated microbiota may obscure the response of intestinal microbiota to dietary changes. To fully unveil the response of intestinal microbiota to dietary changes, we recommend concurrent profiling of digesta- and mucosa-associated intestinal microbiota whenever it is feasible.

Significant associations between microbial clades and sample metadata

To our knowledge, only a few studies have carried out association analysis between intestinal microbial clades and host responses in Atlantic salmon. As such, our results should be treated as preliminary observations and critically evaluated in later studies. Herein, we highlight the significant associations between two mucosa-enriched taxa and host gene expressions in the intestine. Specifically, *B. andersonii*, part of the core microbiota, was associated with the expression of genes related to pro- and anti-inflammatory responses whereas the unclassified *Spirochaetaceae* was associated with the expression of genes related to barrier function. Intestinal microbiota is well known to modulate the local immune responses and intestinal epithelial barrier function (72). Furthermore, it is hypothesized that mucosa-associated microbiota plays a more crucial role in shaping the host immunity in that it can interact both directly and indirectly with intestinal epithelial barrier whereas digesta-associated microbiota can only interact

bioRxiv preprint doi: https://doi.org/10.1101/2020.05.08.083899; this version posted May 9, 2020. The copyright holder for this preprint (which was not certified by peer review) is the author/funder, who has granted bioRxiv a license to display the preprint in perpetuity. It is made available under aCC-BY-ND 4.0 International license.

indirectly (54). Taken together, further research should be undertaken to investigate the potential ecological and functional significance of these two taxa for seawater phase Atlantic salmon.

Quality control: use of mock and negative controls

As in any field of research, conducting a well-controlled microbiome study requires great care in the experiment design such as setting up appropriate experimental controls. The use of mock as a positive control allows for critical evaluation and optimization of microbiota profiling workflow. That all the bacterial taxa in the mock were correctly identified at the genus level indicates that the current workflow is reliable for the taxonomic profiling of intestinal microbiota. Furthermore, the taxonomic profile of mock from different DNA extraction batches was fairly similar, suggesting that the results generated by the current workflow are also largely reproducible. However, the low concordance between the expected and observed relative abundance of bacterial taxa in the mock is reminiscent of the fact that bias is introduced at different steps of the marker-gene survey (73-75), among which DNA extraction and PCR amplification are the two largest sources of bias due to preferential extraction and amplification of some microbial clades over others. In line with previous observations that Gram-positive bacteria may be more subjective to incomplete lysis during DNA extraction due to their tough cell walls (76, 77), the recovery of most Gram-positive bacteria in the mock was lower than the expected. The insufficient lysing of Gram-positive bacteria in the mock was largely mitigated in our later experiments by using a mixture of beads with different sizes for the bead beating during DNA extraction (unpublished data). The bias in the marker-gene

bioRxiv preprint doi: https://doi.org/10.1101/2020.05.08.083899; this version posted May 9, 2020. The copyright holder for this preprint (which was not certified by peer review) is the author/funder, who has granted bioRxiv a license to display the preprint in perpetuity. It is made available under aCC-BY-ND 4.0 International license.

sequencing experiments, as reflected in the observed taxonomic profile of the mock, highlights the necessity of validating such results by absolute quantification techniques such as cultivation (if possible), qPCR, flow cytometry and fluorescence *in situ* hybridization.

Reagent contamination is a common issue in molecular-based studies of microbial communities. The main contaminating taxon identified in this study is *Pseudomonas*, which has been reported as a common reagent contaminant in numerous studies (78-84). Given the dominance of *Pseudomonas* in the negative controls of both DNA extraction and PCR, most of the observed contamination has likely derived from PCR reagents such as molecular-grade water (85-87). Notably, *Pseudomonas* has also been isolated from intestinal digesta and mucosa of Atlantic salmon by traditional culturing approaches (71, 88-90), and reported as a member of Atlantic salmon core microbiota in culture-independent studies (19, 23, 33, 34, 38, 91). Due to the low taxonomic resolution of amplicon sequencing, it is difficult to discern contaminating taxa from true signals solely based on taxonomic labels. The inclusion of negative controls, coupled with quantifications of microbial DNA concentration in the samples, has enabled fast and reliable identification of contaminating taxa in this study. Besides *Pseudomonas*, other common reagent contaminants, including *Bradyrhizobium*, *Burkholderia*, *Comamonas*, *Methylobacterium*, *Propionibacterium*, *Ralstonia*, *Sphingomonas* and *Stenotrophomonas* (83, 85, 87, 92-96), have also been frequently reported as members of Atlantic salmon intestinal microbiota, indicating that existing studies of Atlantic salmon intestinal microbiota may have been plagued with reagent contamination that is hard to ascertain

bioRxiv preprint doi: https://doi.org/10.1101/2020.05.08.083899; this version posted May 9, 2020. The copyright holder for this preprint (which was not certified by peer review) is the author/funder, who has granted bioRxiv a license to display the preprint in perpetuity. It is made available under aCC-BY-ND 4.0 International license.

due to lack of negative controls. As reagent contamination is unavoidable, study-specific and can critically influence sequencing-based microbiome analyses (85, 97, 98), negative controls should always be included and sequenced in microbiome studies especially when dealing with low microbial biomass samples like intestinal mucosa.

Conclusion

In summary, we confirmed previous findings in mammals and fish that intestinal digesta and mucosa harbor microbial communities with clear differences. Regardless of diet, microbial richness and diversity were much higher in the digesta than the mucosa. The insect meal diet altered the distal intestinal microbiota assemblage resulting in higher microbial richness and diversity. The diet effect was however dependent on the sample origin, with mucosa-associated intestinal microbiota being more resilient to the dietary change. To fully unveil the response of intestinal microbiota to dietary changes, concurrent profiling of digesta- and mucosa-associated intestinal microbiota is recommended whenever feasible. Lastly, we identified two mucosa-enriched taxa, *Brevinema andersonii* and unclassified *Spirochaetaceae*, which seemed to be associated with the expression in the distal intestine of genes related to immune responses and barrier function, respectively. As mucosa-associated microbiota could play a more critical role in shaping the host metabolism, their potential functional significance for seawater phase Atlantic salmon merits further investigations.

bioRxiv preprint doi: https://doi.org/10.1101/2020.05.08.083899; this version posted May 9, 2020. The copyright holder for this preprint (which was not certified by peer review) is the author/funder, who has granted bioRxiv a license to display the preprint in perpetuity. It is made available under aCC-BY-ND 4.0 International license.

MATERIALS AND METHODS

Experimental fish, diet and sampling

A 16-week seawater feeding trial with Atlantic salmon (initial body weight = 1.40 kg, S.D. = 0.043 kg) was conducted at the Gildeskål Research Station (GIFAS), Nordland, Norway, in accordance with laws regulating the experimentation with live animals in Norway. The experimental fish were randomly assigned into 6 net pens (5 x 5 x 5 m) each containing 90 fish. The fish were fed, in triplicate net pens, either a commercially-relevant reference diet (REF) with a combination of fish meal, soy protein concentrate, pea protein concentrate, corn gluten and wheat gluten as the protein source, or an insect meal diet (IM) wherein all the fish meal and most of the pea protein concentrate were replaced by black soldier fly larvae meal. Fish were fed by hand until apparent satiation once or twice daily depending on the duration of the duration of daylight. During the feeding trial, the water temperature ranged from 7 °C to 13 °C. Further details on the formulation and chemical composition of the diets, and insect meal has been reported elsewhere (31, 32).

At the termination of the feeding trial, 6 fish were randomly taken from each net pen, anesthetized with tricaine methanesulfonate (MS222®; Argent Chemical Laboratories, Redmond, WA, USA) and euthanized by a sharp blow to the head. After cleaning the exterior of each fish with 70% ethanol, the distal intestine, i.e., the segment from the increase in intestinal diameter and the appearance of transverse luminal folds to the anus, was aseptically removed from the abdominal cavity, placed in a sterile Petri dish and opened longitudinally. Only fish with digesta along the whole intestine were sampled to ensure that the intestine had been exposed to the diets. The intestinal digesta was collected

bioRxiv preprint doi: https://doi.org/10.1101/2020.05.08.083899; this version posted May 9, 2020. The copyright holder for this preprint (which was not certified by peer review) is the author/funder, who has granted bioRxiv a license to display the preprint in perpetuity. It is made available under aCC-BY-ND 4.0 International license.

into a 50 mL skirted sterile centrifuge tube and mixed thoroughly using a spatula. An aliquot of the homogenate was then transferred into a 1.5 mL sterile Eppendorf tube and snap-frozen in liquid N_2 for the profiling of digesta-associated intestinal microbiota. A tissue section from the mid part of the distal intestine was excised and rinsed in sterile phosphate-buffered saline 3 times to remove traces of the remaining digesta. After rinsing, the intestinal tissue was longitudinally cut into 3 pieces for histological evaluation (fixed in 4% phosphate-buffered formaldehyde solution for 24 h and transferred to 70% ethanol for storage), RNA extraction (preserved in RNAlater solution and stored at -20 °C) and profiling of mucosa-associated intestinal microbiota (snap-frozen in liquid N_2), respectively. The collection of microbiota samples was performed near a gas burner to secure aseptic conditions. After the sampling of each fish, tools were cleaned and decontaminated by an 70% ethanol spray and flaming. Microbiota samples of the distal intestine digesta (DID) and mucosa (DIM) were transported in dry ice and stored at -80 °C until DNA extraction.

DNA extraction

Total DNA was extracted from ~200 mg distal intestine digesta or mucosa using the QIAamp® DNA Stool Mini Kit (Qiagen, Hilden, Germany; catalog no., 51504) with some modifications to the manufacturer's specifications as described before (19), except that 2 mL prefilled bead tubes (Qiagen; catalog no., 13118-50) were used for the bead beating. For quality control purposes, a companion "blank extraction" sample was added to each batch of sample DNA extraction by omitting the input material, whereas an additional microbial community standard (ZymoBIOMICS™, Zymo Research, California, USA;

bioRxiv preprint doi: https://doi.org/10.1101/2020.05.08.083899; this version posted May 9, 2020. The copyright holder for this preprint (which was not certified by peer review) is the author/funder, who has granted bioRxiv a license to display the preprint in perpetuity. It is made available under aCC-BY-ND 4.0 International license.

465 catalog no., D6300), i.e. mock, was included for each DNA extraction kit as a positive
466 control. The mock consists of 8 bacteria (*Pseudomonas aeruginosa*, *Escherichia coli*,
467 *Salmonella enterica*, *Lactobacillus fermentum*, *Enterococcus faecalis*, *Staphylococcus*
468 *aureus*, *Listeria monocytogenes*, *Bacillus subtilis*) and 2 yeasts (*Saccharomyces*
469 *cerevisiae*, *Cryptococcus neoformans*).

470 **Amplicon PCR**

471 The V1-2 hypervariable regions of the bacterial 16S rRNA gene were amplified
472 using the primer set 27F (5'-AGA GTT TGA TCM TGG CTC AG-3') and 338R (5'-GCW
473 GCC WCC CGT AGG WGT-3') (99). The PCR was run in a total reaction volume of 25
474 µL containing 12.5 µL of Phusion® High-Fidelity PCR Master Mix (Thermo Scientific,
475 CA, USA; catalog no., F531L), 10.9 µL molecular grade H_2O, 1 µL DNA template and
476 0.3 µL of each primer (10 µM). The amplification program was set as follows: initial
477 denaturation at 98 °C for 3 min; 35 cycles of denaturation at 98 °C for 15 s, annealing
478 decreasing from 63 °C to 53 °C in 10 cycles for 30 s followed by 25 cycles at 53 °C for
479 30 s, and extension at 72 °C for 30 s; followed by a final extension at 72 °C for 10 min.
480 For samples with faint or invisible bands in the agarose gel after PCR, the PCR condition
481 was optimized by applying serial dilutions to the DNA templates to reduce the influence
482 of PCR inhibitors. All the digesta samples were diluted 1:2 in buffer ATE (10 mM Tris-
483 Cl, pH 8.3, with 0.1 mM EDTA and 0.04% NaN3) whereas all the mucosa samples were
484 diluted 1:32. The formal amplicon PCR was run in duplicate incorporating two negative
485 PCR controls, which were generated by replacing the template DNA with molecular grade
486 H_2O. The duplicate PCR products were then pooled and examined by a 1.5% agarose gel

bioRxiv preprint doi: https://doi.org/10.1101/2020.05.08.083899; this version posted May 9, 2020. The copyright holder for this preprint (which was not certified by peer review) is the author/funder, who has granted bioRxiv a license to display the preprint in perpetuity. It is made available under aCC-BY-ND 4.0 International license.

electrophoresis.

Quantification of 16S rRNA gene by qPCR

To assist in identifying contaminating sequences, the 16S rRNA gene quantity in the diluted DNA templates used for the amplicon PCR was measured by qPCR. The qPCR assays were performed using a universal primer set (forward, 5'-CCA TGA AGT CGG AAT CGC TAG-3'; reverse, 5'-GCT TGA CGG GCG GTG T-3') that has been used for bacterial DNA quantification in previous studies (100, 101). The assays were carried out using the LightCycler 96 (Roche Applied Science, Basel, Switzerland) in a 10 μL reaction volume, which contained 2 μL of PCR-grade water, 1 μL diluted DNA template, 5 μL LightCycler 480 SYBR Green I Master Mix (Roche Applied Science) and 1 μL (3 μM) of each primer. Samples, together with the extraction blanks and mock, were run in duplicate in addition to Femto™ bacterial DNA standards (Zymo Research; catalog no., E2006) and a no-template control of the qPCR assay. The qPCR program encompassed an initial enzyme activation step at 95 °C for 2 min, 45 three-step cycles of 95 °C for 10 s, 60 °C for 30 s and 72 °C for 15 s, and a melting curve analysis at the end. Quantification cycle (Cq) values were determined using the second derivative method (102). The specificity of qPCR amplification was confirmed by evaluating the melting curve of qPCR products and the band pattern on the agarose gel after electrophoresis. The inter-plate calibration factor was calculated following the method described in (103), using the bacterial DNA standards as inter-plate calibrators.

Sequencing

The sequencing was carried out on a Miseq platform following the Illumina 16S

bioRxiv preprint doi: https://doi.org/10.1101/2020.05.08.083899; this version posted May 9, 2020. The copyright holder for this preprint (which was not certified by peer review) is the author/funder, who has granted bioRxiv a license to display the preprint in perpetuity. It is made available under aCC-BY-ND 4.0 International license.

metagenomic sequencing library preparation protocol (104). Briefly, the PCR products were cleaned using the Agencourt AMPure XP system (Beckman Coulter, Indiana, USA; catalog no., A63881), multiplexed by dual indexing using the Nextera XT Index Kit (Illumina, California, USA; catalog no., FC-131-1096) and purified again using the AMPure beads. After the second clean-up, representative libraries were selected and analyzed using the Agilent DNA 1000 Kit (Agilent Technologies, California, USA; catalog no., 5067-1505) to verify the library size. Cleaned libraries were quantified using the Invitrogen Qubit™ dsDNA HS Assay Kit (Thermo Fisher Scientific, California, USA; catalog no., Q32854), diluted to 4 nM in 10 mM Tris (pH 8.5) and finally pooled in an equal volume. Negative controls with library concentrations lower than 4 nM were pooled in equal volume directly. Due to the low diversity of amplicon library, 15% Illumina generated PhiX control (catalog no., FC-110-3001) was spiked in by combining 510 μL amplicon library with 90 μL PhiX control library. The library was loaded at 6 pM and sequenced using the Miseq Reagent Kit v3 (600-cycle) (Illumina; catalog no., MS-102-3003).

Sequence data processing

The raw sequence data were processed by the DADA2 1.14 in R 3.6.3 (105) to infer amplicon sequence variants (ASVs) (106). Specifically, the demultiplexed paired-ended reads were trimmed off the primer sequences (forward reads, first 20 bps; reverse reads, first 18 bps), truncated at the position where the median Phred quality score crashed (forward reads, at position 290 bp; reverse reads, at position 248 bp) and filtered off low-quality reads. After trimming and filtering, the run-specific error rates were estimated and

bioRxiv preprint doi: https://doi.org/10.1101/2020.05.08.083899; this version posted May 9, 2020. The copyright holder for this preprint (which was not certified by peer review) is the author/funder, who has granted bioRxiv a license to display the preprint in perpetuity. It is made available under aCC-BY-ND 4.0 International license.

the ASVs were inferred by pooling reads from all the samples sequenced in the same run. The chimeras were removed using the "pooled" method after merging the reads. The resulting raw ASV table and representative sequences were imported into QIIME2 (version, 2020.2) (107). The taxonomy was assigned by a scikit-learn naive Bayes machine-learning classifier (108), which was trained on the SILVA 132 99% OTUs (109) that were trimmed to only include the regions of 16S rRNA gene amplified by our primers. Taxa identified as chloroplasts or mitochondria were excluded from the ASV table. The ASV table was conservatively filtered to remove ASVs that had no phylum-level taxonomic assignment or appeared in only one biological sample. Contaminating ASVs were identified based on two suggested criteria: contaminants are often found in negative controls and inversely correlate with sample DNA concentration (84). The ASVs filtered from the raw ASV table were also removed from the representative sequences, which were then inserted into a reference phylogenetic tree built on the SILVA 128 database using SEPP (110). The alpha rarefaction curves and the core metrics results were generated with a sampling depth of 10000 and 2047 sequences per sample, respectively. For downstream data analysis and visualization, QIIME2 artifacts were imported into R using the *qiime2R* package (111) and a *phyloseq* (112) object was assembled from the sample metadata, ASV table, taxonomy and phylogenetic tree. The core microbiota and alpha-diversity indices were computed using the ASV table collapsed at the species level. The core microbiota was calculated based on the 80% prevalence threshold and visualized by the Venn's diagram. The alpha-diversity indices, including observed species, Pielou's evenness, Shannon's index and Faith's phylogenetic diversity (PD), were computed via

bioRxiv preprint doi: https://doi.org/10.1101/2020.05.08.083899; this version posted May 9, 2020. The copyright holder for this preprint (which was not certified by peer review) is the author/funder, who has granted bioRxiv a license to display the preprint in perpetuity. It is made available under aCC-BY-ND 4.0 International license.

the R packages *microbiome* (113) and *picante* (114). For beta-diversity analyses, we used distance matrices including Jaccard distance, unweighted UniFrac distance, Aitchison distance and phylogenetic isometric log-ratio (PHILR) transformed Euclidean distance. Since rarefying remains to be the best solution for unweighted distance matrices (115), the Jaccard distance and unweighted UniFrac distance were computed in QIIME2 using the rarefied ASV table. The compositionality-aware distance matrices, Aitchison distance and PHILR transformed Euclidean distance, were calculated using the unrarefied ASV table. The Aitchison distance was computed by the *DEICODE* plugin in QIIME2, a form of Aitchison distance that is robust to high levels of sparsity by using the matrix completion to handle the excessive zeros in the microbiome data (116). The PHILR transform of the ASV table was performed in R using the *philr* package (117). The selected distance matrices were explored and visualized by the principal coordinates analysis (PCoA).

Multivariate association analysis

The ASV table was collapsed at the genus level before running the multivariate association analysis. Bacterial taxa of very low abundance (< 0.01%) or low prevalence (present in < 25% of samples) were removed from the feature table. The microbial clades were then tested for significant associations with metadata of interest by MaAsLin2 (version, 0.99.12) (https://huttenhower.sph.harvard.edu/maaslin2) in R, using the default parameters. The results of the analysis are the associations of specific microbial clades with metadata, deconfounding the influence of other factors included in the model. Association was considered significant when the *q*-value was below 0.25. Metadata

bioRxiv preprint doi: https://doi.org/10.1101/2020.05.08.083899; this version posted May 9, 2020. The copyright holder for this preprint (which was not certified by peer review) is the author/funder, who has granted bioRxiv a license to display the preprint in perpetuity. It is made available under aCC-BY-ND 4.0 International license.

575 included in the multivariate association testing are fixed factors Diet + Sample origin +
576 distal intestine somatic index (DISI) + lamina propria cellularity (histological scores) +
577 immune response (qPCR) + barrier function (qPCR), and random factors FishID +
578 NetPen. FishID was nested in NetPen, and NetPen nested in Diet. Lamina propria
579 cellularity reflects the severity of inflammation in the distal intestine. Based on the degree
580 of cellular infiltration within the lamina propria, a value of normal, mild, moderate,
581 marked or severe was assigned. To make the data appropriate for the association testing,
582 the highly skewed five-category scores were collapsed into more balanced binary data,
583 i.e., normal and abnormal. The immune-related genes included for the association testing
584 were myeloid differentiation factor 88 (*myd88*), interleukin 1β (*il1β*), interleukin 8 (*il8*),
585 cluster of differentiation 3 γδ (*cd3γδ*), transforming growth factor β1 (*tgfβ1*), interferon γ
586 (*ifnγ*), interleukin 17A (*il17a*), fork-head box P3 (*foxp3*) and interleukin 10 (*il10*), whose
587 expression levels were higher in the distal intestine of fish assigned abnormal regarding
588 lamina propria cellularity. Since the expression levels of immune-related genes were
589 highly correlated, we ran a principal component analysis (PCA) and extracted the first
590 principle component (PC1) for the association testing to avoid multicollinearity and
591 reduce the number of association testing. For genes relevant to the barrier function, which
592 included claudin-15 (*cldn15*), claudin-25b (*cldn25b*), zonula occludens 1 (*zo1*), E-
593 cadherin / cadherin 1 (*cdh1*) and mucin-2 (*muc2*), we also used the PC1 of the PCA for
594 the association testing based on the same considerations.

595 **Statistics**

596 All the statistical analyses were run in R except for the PERMANOVA, which was

bioRxiv preprint doi: https://doi.org/10.1101/2020.05.08.083899; this version posted May 9, 2020. The copyright holder for this preprint (which was not certified by peer review) is the author/funder, who has granted bioRxiv a license to display the preprint in perpetuity. It is made available under aCC-BY-ND 4.0 International license.

run in PRIMER v7. The differences in the alpha-diversity indices were compared using linear mixed-effects models via the *lme4* package (118). Predictor variables in the models included the fixed effects Diet + Sample origin + Diet x Sample origin, and the random effects FishID + NetPen. The models were validated by visual inspections of residual diagnostic plots generated by the *ggResidpanel* package (119). The statistical significance of fixed predictors was estimated by Type III *ANOVA* with Kenward-Roger's approximation of denominator degrees of freedom via the *lmerTest* package (120). When the interaction between the main effects was significant, conditional contrasts for the main effects were made via the *emmeans* package (121). To compare the differences in beta-diversity, we performed the PERMANOVA (122) using the same predictors included in the linear mixed-effects models. Terms with negative estimates for components of variation were sequentially removed from the model via term pooling, starting with the one showing the smallest mean squares. At each step, the model was reassessed whether more terms need to be removed or not. Conditional contrasts for the main effects were constructed when their interaction was significant. Monte Carlo *p* values were computed as well when the unique permutations for the terms in the PERMANOVA were small (< 100). The homogeneity of multivariate dispersions among groups was visually assessed with boxplots and was formally tested by the permutation test, PERMDISP (123), via the R package *vegan* (124). Multiple comparisons were adjusted by the Benjamini-Hochberg procedure where applicable. Differences were regarded as significant when $p < 0.05$.

Code availability

All the code for reproducing the results are available from the GitHub repository

bioRxiv preprint doi: https://doi.org/10.1101/2020.05.08.083899; this version posted May 9, 2020. The copyright holder for this preprint (which was not certified by peer review) is the author/funder, who has granted bioRxiv a license to display the preprint in perpetuity. It is made available under aCC-BY-ND 4.0 International license.

(https://github.com/yanxianl/Li_AqFl2-Microbiota_ASM_2020).

Data availability

Raw sequence data are deposited at the NCBI SRA database (https://www.ncbi.nlm.nih.gov/sra) under the BioProject PRJNA555355. Other raw data and sample metadata are available from the GitHub repository (https://github.com/yanxianl/Li_AqFl2-Microbiota_ASM_2020).

ACKNOWLEDGMENTS

Y.L. was granted a scholarship from the China Scholarship Council to pursue his PhD degree at Norwegian University of Life Sciences. This work was a spin-off of the "AquaFly" project (grant number, 238997), funded by the Research Council of Norway and managed by the Institute of Marine Research. Costs related to this study were covered by Norwegian University of Life Sciences. The funding agencies had no role in study design, data collection and interpretation, decision to publish or preparation of the manuscript.

The authors wish to thank Ellen K. Hage for organizing the sampling and technicians at the GIFAS for their committed animal care and supports during the sampling.

T.M.K. and Å.K. concepted and designed the study. Y.L., L.B. and K.G. participated in the sample collection. Y.L., L.B. and A.J.-T. carried out the laboratory works. Y.L. performed the bioinformatics, statistical analyses and data visualization. Y.L. and L.B. completed the first draft of the manuscript. All the authors read, revised and approved the final version of the manuscript.

bioRxiv preprint doi: https://doi.org/10.1101/2020.05.08.083899; this version posted May 9, 2020. The copyright holder for this preprint (which was not certified by peer review) is the author/funder, who has granted bioRxiv a license to display the preprint in perpetuity. It is made available under aCC-BY-ND 4.0 International license.

We declare no conflicts of interest.

REFERENCE

1. Ray A, Ghosh K, Ringø E. 2012. Enzyme-producing bacteria isolated from fish gut: a review. Aquac Nutr 18:465-492.
2. Falcinelli S, Picchietti S, Rodiles A, Cossignani L, Merrifield DL, Taddei AR, Maradonna F, Olivotto I, Gioacchini G, Carnevali O. 2015. *Lactobacillus rhamnosus* lowers zebrafish lipid content by changing gut microbiota and host transcription of genes involved in lipid metabolism. Sci Rep 5:9336.
3. Semova I, Carten JD, Stombaugh J, Mackey LC, Knight R, Farber SA, Rawls JF. 2012. Microbiota regulate intestinal absorption and metabolism of fatty acids in the zebrafish. Cell Host Microbe 12:277-288.
4. Lyte M, Cryan JF. 2014. Microbial endocrinology: the microbiota-gut-brain axis in health and disease, vol 817. Springer.
5. Jeon SR, Chai J, Kim C, Lee CH. 2018. Current evidence for the management of inflammatory bowel diseases using fecal microbiota transplantation. Curr Infect Dis Rep 20:21.
6. Frank DN, St Amand AL, Feldman RA, Boedeker EC, Harpaz N, Pace NR. 2007. Molecular-phylogenetic characterization of microbial community imbalances in human inflammatory bowel diseases. Proc Natl Acad Sci U S A 104:13780-5.
7. Manichanh C, Rigottier-Gois L, Bonnaud E, Gloux K, Pelletier E, Frangeul L, Nalin R, Jarrin C, Chardon P, Marteau P. 2006. Reduced diversity of faecal

bioRxiv preprint doi: https://doi.org/10.1101/2020.05.08.083899; this version posted May 9, 2020. The copyright holder for this preprint (which was not certified by peer review) is the author/funder, who has granted bioRxiv a license to display the preprint in perpetuity. It is made available under aCC-BY-ND 4.0 International license.

microbiota in Crohn's disease revealed by a metagenomic approach. Gut 55:205-211.

8. Narula N, Kassam Z, Yuan Y, Colombel JF, Ponsioen C, Reinisch W, Moayyedi P. 2017. Systematic review and meta-analysis: fecal microbiota transplantation for treatment of active ulcerative colitis. Inflamm Bowel Dis 23:1702-1709.

9. Wu GD, Chen J, Hoffmann C, Bittinger K, Chen YY, Keilbaugh SA, Bewtra M, Knights D, Walters WA, Knight R, Sinha R, Gilroy E, Gupta K, Baldassano R, Nessel L, Li H, Bushman FD, Lewis JD. 2011. Linking long-term dietary patterns with gut microbial enterotypes. Science 334:105-8.

10. Muegge BD, Kuczynski J, Knights D, Clemente JC, González A, Fontana L, Henrissat B, Knight R, Gordon JI. 2011. Diet drives convergence in gut microbiome functions across mammalian phylogeny and within humans. Science 332:970-974.

11. De Filippo C, Cavalieri D, Di Paola M, Ramazzotti M, Poullet JB, Massart S, Collini S, Pieraccini G, Lionetti P. 2010. Impact of diet in shaping gut microbiota revealed by a comparative study in children from Europe and rural Africa. Proc Natl Acad Sci U S A 107:14691-6.

12. David LA, Maurice CF, Carmody RN, Gootenberg DB, Button JE, Wolfe BE, Ling AV, Devlin AS, Varma Y, Fischbach MA, Biddinger SB, Dutton RJ, Turnbaugh PJ. 2014. Diet rapidly and reproducibly alters the human gut microbiome. Nature 505:559-63.

13. Wang Z, Klipfell E, Bennett BJ, Koeth R, Levison BS, Dugar B, Feldstein AE,

bioRxiv preprint doi: https://doi.org/10.1101/2020.05.08.083899; this version posted May 9, 2020. The copyright holder for this preprint (which was not certified by peer review) is the author/funder, who has granted bioRxiv a license to display the preprint in perpetuity. It is made available under aCC-BY-ND 4.0 International license.

683 Britt EB, Fu X, Chung YM, Wu Y, Schauer P, Smith JD, Allayee H, Tang WH,
684 DiDonato JA, Lusis AJ, Hazen SL. 2011. Gut flora metabolism of
685 phosphatidylcholine promotes cardiovascular disease. Nature 472:57-63.
686 14. Hryckowian AJ, Van Treuren W, Smits SA, Davis NM, Gardner JO, Bouley DM,
687 Sonnenburg JL. 2018. Microbiota-accessible carbohydrates suppress *Clostridium*
688 *difficile* infection in a murine model. Nat Microbiol 3:662-669.
689 15. FAO. 2018. The State of World Fisheries and Aquaculture. FAO, Rome, Italy.
690 16. Aas TS, Ytrestøyl T, Åsgård T. 2019. Utilization of feed resources in the
691 production of Atlantic salmon (*Salmo salar*) in Norway: An update for 2016.
692 Aquac Rep 15:100216.
693 17. Sánchez-Muros M-J, Barroso FG, Manzano-Agugliaro F. 2014. Insect meal as
694 renewable source of food for animal feeding: a review. J Clean Prod 65:16-27.
695 18. Øverland M, Skrede A. 2016. Yeast derived from lignocellulosic biomass as a
696 sustainable feed resource for use in aquaculture. J Sci Food Agric 97:733-742.
697 19. Gajardo K, Jaramillo-Torres A, Kortner TM, Merrifield DL, Tinsley J, Bakke AM,
698 Krogdahl Å. 2017. Alternative protein sources in the diet modulate microbiota and
699 functionality in the distal intestine of Atlantic salmon (*Salmo salar*). Appl Environ
700 Microbiol 83:e02615-16.
701 20. Jin Y, Angell IL, Rod Sandve S, Snipen LG, Olsen Y, Rudi K. 2019. Atlantic
702 salmon raised with diets low in long-chain polyunsaturated n-3 fatty acids in
703 freshwater have a *Mycoplasma*-dominated gut microbiota at sea. Aquac Environ
704 Interact 11:31-39.

bioRxiv preprint doi: https://doi.org/10.1101/2020.05.08.083899; this version posted May 9, 2020. The copyright holder for this preprint (which was not certified by peer review) is the author/funder, who has granted bioRxiv a license to display the preprint in perpetuity. It is made available under aCC-BY-ND 4.0 International license.

21. Schmidt V, Amaral-Zettler L, Davidson J, Summerfelt S, Good C. 2016. Influence of fishmeal-free diets on microbial communities in Atlantic salmon (*Salmo salar*) recirculation aquaculture systems. Appl Environ Microbiol 82:4470-4481.

22. Eckburg PB, Bik EM, Bernstein CN, Purdom E, Dethlefsen L, Sargent M, Gill SR, Nelson KE, Relman DA. 2005. Diversity of the human intestinal microbial flora. Science 308:1635-8.

23. Gajardo K, Rodiles A, Kortner TM, Krogdahl Å, Bakke AM, Merrifield DL, Sorum H. 2016. A high-resolution map of the gut microbiota in Atlantic salmon (*Salmo salar*): A basis for comparative gut microbial research. Sci Rep 6:30893.

24. Looft T, Allen HK, Cantarel BL, Levine UY, Bayles DO, Alt DP, Henrissat B, Stanton TB. 2014. Bacteria, phages and pigs: the effects of in-feed antibiotics on the microbiome at different gut locations. ISME J 8:1566.

25. Lyons PP, Turnbull JF, Dawson KA, Crumlish M. 2017. Exploring the microbial diversity of the distal intestinal lumen and mucosa of farmed rainbow trout *Oncorhynchus mykiss* (Walbaum) using next generation sequencing (NGS). Aquac Res 48:77-91.

26. Huyben D, Sun L, Moccia R, Kiessling A, Dicksved J, Lundh T. 2018. Dietary live yeast and increased water temperature influence the gut microbiota of rainbow trout. J Appl Microbiol 124:1377-1392.

27. Jaramillo-Torres A, Rawling MD, Rodiles A, Mikalsen HE, Johansen LH, Tinsley J, Forberg T, Aasum E, Castex M, Merrifield DL. 2019. Influence of Dietary Supplementation of Probiotic *Pediococcus acidilactici* MA18/5M During the

bioRxiv preprint doi: https://doi.org/10.1101/2020.05.08.083899; this version posted May 9, 2020. The copyright holder for this preprint (which was not certified by peer review) is the author/funder, who has granted bioRxiv a license to display the preprint in perpetuity. It is made available under aCC-BY-ND 4.0 International license.

Transition From Freshwater to Seawater on Intestinal Health and Microbiota of Atlantic Salmon (*Salmo salar* L.). Front Microbiol 10:2243.

28. Rimoldi S, Gini E, Iannini F, Gasco L, Terova G. 2019. The effects of dietary insect meal from *Hermetia illucens* prepupae on autochthonous gut microbiota of rainbow trout (*Oncorhynchus mykiss*). Animals (Basel) 9.

29. Terova G, Rimoldi S, Ascione C, Gini E, Ceccotti C, Gasco L. 2019. Rainbow trout (*Oncorhynchus mykiss*) gut microbiota is modulated by insect meal from *Hermetia illucens* prepupae in the diet. Rev Fish Biol Fish 29:465-486.

30. Bruni L, Belghit I, Lock EJ, Secci G, Taiti C, Parisi GA. 2020. Total replacement of dietary fish meal with black soldier fly (*Hermetia illucens*) larvae does not impair physical, chemical or volatile composition of farmed Atlantic salmon (*Salmo salar* L.). J Sci Food Agric 100:1038-1047.

31. Li Y, Kortner TM, Chikwati EM, Belghit I, Lock E-J, Krogdahl Å. 2020. Total replacement of fish meal with black soldier fly (*Hermetia illucens*) larvae meal does not compromise the gut health of Atlantic salmon (*Salmo salar*). Aquaculture 520:734967.

32. Belghit I, Liland NS, Gjesdal P, Biancarosa I, Menchetti E, Li Y, Waagbø R, Krogdahl Å, Lock E-J. 2019. Black soldier fly larvae meal can replace fish meal in diets of sea-water phase Atlantic salmon (*Salmo salar*). Aquaculture 503:609-619.

33. Dehler CE, Secombes CJ, Martin SA. 2017. Seawater transfer alters the intestinal microbiota profiles of Atlantic salmon (*Salmo salar* L.). Sci Rep 7:13877.

bioRxiv preprint doi: https://doi.org/10.1101/2020.05.08.083899; this version posted May 9, 2020. The copyright holder for this preprint (which was not certified by peer review) is the author/funder, who has granted bioRxiv a license to display the preprint in perpetuity. It is made available under aCC-BY-ND 4.0 International license.

34. Dehler CE, Secombes CJ, Martin SAM. 2017. Environmental and physiological factors shape the gut microbiota of Atlantic salmon parr (*Salmo salar* L.). Aquaculture 467:149-157.

35. Gupta S, Feckaninova A, Lokesh J, Koscova J, Sorensen M, Femandes J, Kiron V. 2019. *Lactobacillus* dominate in the intestine of Atlantic salmon fed dietary probiotics. Front Microbiol 9.

36. Gupta S, Lokesh J, Abdelhafiz Y, Siriyappagouder P, Pierre R, Sorensen M, Fernandes JMO, Kiron V. 2019. Macroalga-derived alginate oligosaccharide alters intestinal bacteria of Atlantic salmon. Front Microbiol 10.

37. Llewellyn MS, McGinnity P, Dionne M, Letourneau J, Thonier F, Carvalho GR, Creer S, Derome N. 2015. The biogeography of the Atlantic salmon (*Salmo salar*) gut microbiome. ISME J 10:1280-1284.

38. Webster TMU, Consuegra S, Hitchings M, de Leaniz CG. 2018. Interpopulation variation in the Atlantic salmon microbiome reflects environmental and genetic diversity. Appl Environ Microbiol 84:e00691-18.

39. Fogarty C, Burgess CM, Cotter PD, Cabrera-Rubio R, Whyte P, Smyth C, Bolton DJ. 2019. Diversity and composition of the gut microbiota of Atlantic salmon (*Salmo salar*) farmed in Irish waters. J Appl Microbiol 127:648-657.

40. Godoy FA, Miranda CD, Wittwer GD, Aranda CP, Calderon R. 2015. High variability of levels of *Aliivibrio* and lactic acid bacteria in the intestinal microbiota of farmed Atlantic salmon *Salmo salar* L. Ann Microbiol 65:2343-2353.

bioRxiv preprint doi: https://doi.org/10.1101/2020.05.08.083899; this version posted May 9, 2020. The copyright holder for this preprint (which was not certified by peer review) is the author/funder, who has granted bioRxiv a license to display the preprint in perpetuity. It is made available under aCC-BY-ND 4.0 International license.

41. Karlsen C, Ottem K, Brevik ØJ, Davey M, Sørum H, Winther-Larsen H. 2017. The environmental and host-associated bacterial microbiota of Arctic seawater-farmed Atlantic salmon with ulcerative disorders. J Fish Dis 40:1645-1663.

42. Zarkasi KZ, Abell GCJ, Taylor RS, Neuman C, Hatje E, Tamplin ML, Katouli M, Bowman JP. 2014. Pyrosequencing-based characterization of gastrointestinal bacteria of Atlantic salmon (*Salmo salar* L.) within a commercial mariculture system. J Appl Microbiol 117:18-27.

43. Zarkasi KZ, Taylor RS, Abell GC, Tamplin ML, Glencross BD, Bowman JP. 2016. Atlantic salmon (*Salmo salar* L.) gastrointestinal microbial community dynamics in relation to digesta properties and diet. Microb Ecol 71:589-603.

44. Urbanczyk H, Ast JC, Higgins MJ, Carson J, Dunlap PV. 2007. Reclassification of *Vibrio fischeri*, *Vibrio logei*, *Vibrio salmonicida* and *Vibrio wodanis* as *Aliivibrio fischeri* gen. nov., comb. nov., *Aliivibrio logei* comb. nov., *Aliivibrio salmonicida* comb. nov. and *Aliivibrio wodanis* comb. nov. Int J Syst Evol Microbiol 57:2823-2829.

45. Dunlap PV, Ast JC, Kimura S, Fukui A, Yoshino T, Endo H. 2007. Phylogenetic analysis of host–symbiont specificity and codivergence in bioluminescent symbioses. Cladistics 23:507-532.

46. Egidius E, Wiik R, Andersen K, Hoff K, Hjeltnes B. 1986. *Vibrio salmonicida* sp. nov., a new fish pathogen. Int J Syst Evol Microbiol 36:518-520.

47. Lunder T, Sørum H, Holstad G, Steigerwalt AG, Mowinckel P, Brenner DJ. 2000. Phenotypic and genotypic characterization of *Vibrio viscosus* sp. nov. and *Vibrio*

bioRxiv preprint doi: https://doi.org/10.1101/2020.05.08.083899; this version posted May 9, 2020. The copyright holder for this preprint (which was not certified by peer review) is the author/funder, who has granted bioRxiv a license to display the preprint in perpetuity. It is made available under aCC-BY-ND 4.0 International license.

wodanis sp. nov. isolated from Atlantic salmon (*Salmo salar*) with'winter ulcer'. Int J Syst Evol Microbiol 50:427-450.

48. Anderson JF, Johnson RC, Magnarelli LA, Hyde FW, Andreadis TG. 1987. New infectious spirochete isolated from short-tailed shrews and white-footed mice. J Clin Microbiol 25:1490-4.

49. Brown RM, Wiens GD, Salinas I. 2019. Analysis of the gut and gill microbiome of resistant and susceptible lines of rainbow trout (*Oncorhynchus mykiss*). Fish Shellfish Immunol 86:497-506.

50. Tapia-Paniagua S, Vidal S, Lobo C, Prieto-Álamo M, Jurado J, Cordero H, Cerezuela R, de la Banda IG, Esteban M, Balebona M. 2014. The treatment with the probiotic *Shewanella putrefaciens* Pdp11 of specimens of *Solea senegalensis* exposed to high stocking densities to enhance their resistance to disease. Fish Shellfish Immunol 41:209-221.

51. Holben W, Williams P, Saarinen M, Särkilahti L, Apajalahti J. 2002. Phylogenetic analysis of intestinal microflora indicates a novel *Mycoplasma* phylotype in farmed and wild salmon. Microb Ecol 44:175-185.

52. Razin S, Yogev D, Naot Y. 1998. Molecular biology and pathogenicity of mycoplasmas. Microbiol Mol Biol Rev 62:1094-156.

53. Pollack JD, Williams MV, McElhaney RN. 1997. The comparative metabolism of the mollicutes (*Mycoplasmas*): the utility for taxonomic classification and the relationship of putative gene annotation and phylogeny to enzymatic function in the smallest free-living cells. Crit Rev Microbiol 23:269-354.

bioRxiv preprint doi: https://doi.org/10.1101/2020.05.08.083899; this version posted May 9, 2020. The copyright holder for this preprint (which was not certified by peer review) is the author/funder, who has granted bioRxiv a license to display the preprint in perpetuity. It is made available under aCC-BY-ND 4.0 International license.

54. Van den Abbeele P, Van de Wiele T, Verstraete W, Possemiers S. 2011. The host selects mucosal and luminal associations of coevolved gut microorganisms: a novel concept. FEMS Microbiol Rev 35:681-704.

55. Kennedy M, Rosnick D, Ulrich R, Yancey Jr R. 1988. Association of *Treponema hyodysenteriae* with porcine intestinal mucosa. J Gen Microbiol 134:1565-1576.

56. Milner J, Sellwood R. 1994. Chemotactic response to mucin by *Serpulina hyodysenteriae* and other porcine spirochetes: potential role in intestinal colonization. Infect Immun 62:4095-4099.

57. Witters NA, Duhamel GE. 1999. Motility-regulated mucin association of *Serpulina pilosicoli*, the agent of colonic spirochetosis of humans and animals, p 199-205, Advances in Experimental Medicine and Biology, vol 473. Springer.

58. Bruni L, Pastorelli R, Viti C, Gasco L, Parisi G. 2018. Characterisation of the intestinal microbial communities of rainbow trout (*Oncorhynchus mykiss*) fed with *Hermetia illucens* (black soldier fly) partially defatted larva meal as partial dietary protein source. Aquaculture 487:56-63.

59. Huyben D, Vidaković A, Hallgren SW, Langeland M. 2019. High-throughput sequencing of gut microbiota in rainbow trout (*Oncorhynchus mykiss*) fed larval and pre-pupae stages of black soldier fly (*Hermetia illucens*). Aquaculture 500:485-491.

60. Borrelli L, Coretti L, Dipineto L, Bovera F, Menna F, Chiariotti L, Nizza A, Lembo F, Fioretti A. 2017. Insect-based diet, a promising nutritional source, modulates gut microbiota composition and SCFAs production in laying hens. Sci

bioRxiv preprint doi: https://doi.org/10.1101/2020.05.08.083899; this version posted May 9, 2020. The copyright holder for this preprint (which was not certified by peer review) is the author/funder, who has granted bioRxiv a license to display the preprint in perpetuity. It is made available under aCC-BY-ND 4.0 International license.

Rep 7:1-11.

61. Kawasaki K, Hashimoto Y, Hori A, Kawasaki T, Hirayasu H, Iwase S, Hashizume A, Ido A, Miura C, Miura T, Nakamura S, Seyama T, Matsumoto Y, Kasai K, Fujitani Y. 2019. Evaluation of black soldier fly (*Hermetia illucens*) larvae and pre-pupae raised on household organic waste, as potential ingredients for poultry feed. Animals (Basel) 9.

62. Jozefiak A, Nogales-Merida S, Mikolajczak Z, Rawski M, Kieronczyk B, Mazurkiewicz J. 2019. The utilization of full-fat insect meal in rainbow trout (*oncorhynchus mykiss*) nutrition: The effects on growth performance, intestinal microbiota and gastrointestinal tract histomorphology. Ann Anim Sci 19:747-765.

63. Jozefiak A, Nogales-Merida S, Rawski M, Kieronczyk B, Mazurkiewicz J. 2019. Effects of insect diets on the gastrointestinal tract health and growth performance of Siberian sturgeon (*Acipenser baerii* Brandt, 1869). BMC Microbiol 15.

64. Jiang CL, Jin WZ, Tao XH, Zhang Q, Zhu J, Feng SY, Xu XH, Li HY, Wang ZH, Zhang ZJ. 2019. Black soldier fly larvae (*Hermetia illucens*) strengthen the metabolic function of food waste biodegradation by gut microbiome. Microb Biotechnol 12:528-543.

65. Bruno D, Bonelli M, De Filippis F, Di Lelio I, Tettamanti G, Casartelli M, Ercolini D, Caccia S. 2019. The intestinal microbiota of *Hermetia illucens* larvae is affected by diet and shows a diverse composition in the different midgut regions. Appl Environ Microbiol 85:e01864-18.

66. Wynants E, Frooninckx L, Crauwels S, Verreth C, De Smet J, Sandrock C,

bioRxiv preprint doi: https://doi.org/10.1101/2020.05.08.083899; this version posted May 9, 2020. The copyright holder for this preprint (which was not certified by peer review) is the author/funder, who has granted bioRxiv a license to display the preprint in perpetuity. It is made available under aCC-BY-ND 4.0 International license.

Wohlfahrt J, Van Schelt J, Depraetere S, Lievens B. 2019. Assessing the microbiota of black soldier fly larvae (*Hermetia illucens*) reared on organic waste streams on four different locations at laboratory and large scale. Microb Ecol 77:913-930.

67. Zheng L, Crippen TL, Singh B, Tarone AM, Dowd S, Yu Z, Wood TK, Tomberlin JK. 2013. A survey of bacterial diversity from successive life stages of black soldier fly (Diptera: Stratiomyidae) by using 16S rDNA pyrosequencing. J Med Entomol 50:647-658.

68. Emerson JB, Adams RI, Roman CMB, Brooks B, Coil DA, Dahlhausen K, Ganz HH, Hartmann EM, Hsu T, Justice NB, Paulino-Lima IG, Luongo JC, Lymperopoulou DS, Gomez-Silvan C, Rothschild-Mancinelli B, Balk M, Huttenhower C, Nocker A, Vaishampayan P, Rothschild LJ. 2017. Schrodinger's microbes: Tools for distinguishing the living from the dead in microbial ecosystems. Microbiome 5:86.

69. Beier S, Bertilsson S. 2013. Bacterial chitin degradation—mechanisms and ecophysiological strategies. Front Microbiol 4:149.

70. Cody R. 1989. Distribution of chitinase and chitobiase in *Bacillus*. Curr Microbiol 19:201-205.

71. Askarian F, Zhou ZG, Olsen RE, Sperstad S, Ringo E. 2012. Culturable autochthonous gut bacteria in Atlantic salmon (*Salmo salar* L.) fed diets with or without chitin. Characterization by 16S rRNA gene sequencing, ability to produce enzymes and in vitro growth inhibition of four fish pathogens. Aquaculture 326:1-

bioRxiv preprint doi: https://doi.org/10.1101/2020.05.08.083899; this version posted May 9, 2020. The copyright holder for this preprint (which was not certified by peer review) is the author/funder, who has granted bioRxiv a license to display the preprint in perpetuity. It is made available under aCC-BY-ND 4.0 International license.

8.

72. Maynard CL, Elson CO, Hatton RD, Weaver CT. 2012. Reciprocal interactions of the intestinal microbiota and immune system. Nature 489:231-41.

73. McLaren MR, Willis AD, Callahan BJ. 2019. Consistent and correctable bias in metagenomic sequencing experiments. Elife 8.

74. Brooks JP, Edwards DJ, Harwich MD, Rivera MC, Fettweis JM, Serrano MG, Reris RA, Sheth NU, Huang B, Girerd P. 2015. The truth about metagenomics: quantifying and counteracting bias in 16S rRNA studies. BMC Microbiol 15:66.

75. Sinha R, Abnet CC, White O, Knight R, Huttenhower C. 2015. The microbiome quality control project: baseline study design and future directions. Genome Biol 16:276.

76. Costea PI, Zeller G, Sunagawa S, Pelletier E, Alberti A, Levenez F, Tramontano M, Driessen M, Hercog R, Jung F-E. 2017. Towards standards for human fecal sample processing in metagenomic studies. Nat Biotechnol 35:1069.

77. Santiago A, Panda S, Mengels G, Martinez X, Azpiroz F, Dore J, Guarner F, Manichanh C. 2014. Processing faecal samples: a step forward for standards in microbial community analysis. BMC Microbiol 14:112.

78. Lazarevic V, Gaia N, Girard M, Schrenzel J. 2016. Decontamination of 16S rRNA gene amplicon sequence datasets based on bacterial load assessment by qPCR. BMC Microbiol 16:73.

79. Kim D, Hofstaedter CE, Zhao C, Mattei L, Tanes C, Clarke E, Lauder A, Sherrill-Mix S, Chehoud C, Kelsen J, Conrad M, Collman RG, Baldassano R, Bushman

bioRxiv preprint doi: https://doi.org/10.1101/2020.05.08.083899; this version posted May 9, 2020. The copyright holder for this preprint (which was not certified by peer review) is the author/funder, who has granted bioRxiv a license to display the preprint in perpetuity. It is made available under aCC-BY-ND 4.0 International license.

FD, Bittinger K. 2017. Optimizing methods and dodging pitfalls in microbiome research. Microbiome 5:52.

80. Jousselin E, Clamens AL, Galan M, Bernard M, Maman S, Gschloessl B, Duport G, Meseguer AS, Calevro F, Coeur d'acier A. 2016. Assessment of a 16S rRNA amplicon Illumina sequencing procedure for studying the microbiome of a symbiont-rich aphid genus. Mol Ecol Resour 16:628-40.

81. Jost T, Lacroix C, Braegger C, Chassard C. 2013. Assessment of bacterial diversity in breast milk using culture-dependent and culture-independent approaches. Br J Nutr 110:1253-62.

82. Jervis-Bardy J, Leong LEX, Marri S, Smith RJ, Choo JM, Smith-Vaughan HC, Nosworthy E, Morris PS, O'Leary S, Rogers GB, Marsh RL. 2015. Deriving accurate microbiota profiles from human samples with low bacterial content through post-sequencing processing of Illumina MiSeq data. Microbiome 3:19.

83. Glassing A, Dowd SE, Galandiuk S, Davis B, Chiodini RJ. 2016. Inherent bacterial DNA contamination of extraction and sequencing reagents may affect interpretation of microbiota in low bacterial biomass samples. Gut Pathog 8:24.

84. Davis NM, Proctor DM, Holmes SP, Relman DA, Callahan BJ. 2018. Simple statistical identification and removal of contaminant sequences in marker-gene and metagenomics data. Microbiome 6:226.

85. Salter SJ, Cox MJ, Turek EM, Calus ST, Cookson WO, Moffatt MF, Turner P, Parkhill J, Loman NJ, Walker AW. 2014. Reagent and laboratory contamination can critically impact sequence-based microbiome analyses. BMC Biol 12:87.

bioRxiv preprint doi: https://doi.org/10.1101/2020.05.08.083899; this version posted May 9, 2020. The copyright holder for this preprint (which was not certified by peer review) is the author/funder, who has granted bioRxiv a license to display the preprint in perpetuity. It is made available under aCC-BY-ND 4.0 International license.

86. Kulakov LA, McAlister MB, Ogden KL, Larkin MJ, O'Hanlon JF. 2002. Analysis of bacteria contaminating ultrapure water in industrial systems. Appl Environ Microbiol 68:1548-55.

87. Grahn N, Olofsson M, Ellnebo-Svedlund K, Monstein HJ, Jonasson J. 2003. Identification of mixed bacterial DNA contamination in broad-range PCR amplification of 16S rDNA V1 and V3 variable regions by pyrosequencing of cloned amplicons. FEMS Microbiol Lett 219:87-91.

88. Cantas L, Fraser TWK, Fjelldal PG, Mayer I, Sorum H. 2011. The culturable intestinal microbiota of triploid and diploid juvenile Atlantic salmon (*Salmo salar*) - a comparison of composition and drug resistance. BMC Vet Res 7:71.

89. Navarrete P, Fuentes P, De la Fuente L, Barros L, Magne F, Opazo R, Ibacache C, Espejo R, Romero J. 2013. Short-term effects of dietary soybean meal and lactic acid bacteria on the intestinal morphology and microbiota of Atlantic salmon (*Salmo salar*). Aquac Nutr 19:827-836.

90. Hatje E, Neuman C, Stevenson H, Bowman JP, Katouli M. 2014. Population dynamics of *Vibrio* and *Pseudomonas* species isolated from farmed Tasmanian Atlantic salmon (*Salmo salar* L.): a seasonal study. Microb Ecol 68:679-687.

91. He XP, Chaganti SR, Heath DD. 2018. Population-specific responses to interspecific competition in the gut microbiota of two Atlantic salmon (*Salmo salar*) populations. Microb Ecol 75:140-151.

92. Laurence M, Hatzis C, Brash DE. 2014. Common contaminants in next-generation sequencing that hinder discovery of low-abundance microbes. PLoS

bioRxiv preprint doi: https://doi.org/10.1101/2020.05.08.083899; this version posted May 9, 2020. The copyright holder for this preprint (which was not certified by peer review) is the author/funder, who has granted bioRxiv a license to display the preprint in perpetuity. It is made available under aCC-BY-ND 4.0 International license.

One 9:e97876.

93. Lauder AP, Roche AM, Sherrill-Mix S, Bailey A, Laughlin AL, Bittinger K, Leite R, Elovitz MA, Parry S, Bushman FD. 2016. Comparison of placenta samples with contamination controls does not provide evidence for a distinct placenta microbiota. Microbiome 4:29.

94. Barton HA, Taylor NM, Lubbers BR, Pemberton AC. 2006. DNA extraction from low-biomass carbonate rock: an improved method with reduced contamination and the low-biomass contaminant database. J Microbiol Methods 66:21-31.

95. Weyrich LS, Farrer AG, Eisenhofer R, Arriola LA, Young J, Selway CA, Handsley-Davis M, Adler CJ, Breen J, Cooper A. 2019. Laboratory contamination over time during low-biomass sample analysis. Mol Ecol Resour 19:982-996.

96. Tanner MA, Goebel BM, Dojka MA, Pace NR. 1998. Specific ribosomal DNA sequences from diverse environmental settings correlate with experimental contaminants. Appl Environ Microbiol 64:3110-3.

97. Eisenhofer R, Minich JJ, Marotz C, Cooper A, Knight R, Weyrich LS. 2019. Contamination in low microbial biomass microbiome studies: issues and recommendations. Trends Microbiol 27:105-117.

98. de Goffau MC, Lager S, Salter SJ, Wagner J, Kronbichler A, Charnock-Jones DS, Peacock SJ, Smith GCS, Parkhill J. 2018. Recognizing the reagent microbiome. Nat Microbiol 3:851-853.

99. Roeselers G, Mittge EK, Stephens WZ, Parichy DM, Cavanaugh CM, Guillemin K, Rawls JF. 2011. Evidence for a core gut microbiota in the zebrafish. ISME J

bioRxiv preprint doi: https://doi.org/10.1101/2020.05.08.083899; this version posted May 9, 2020. The copyright holder for this preprint (which was not certified by peer review) is the author/funder, who has granted bioRxiv a license to display the preprint in perpetuity. It is made available under aCC-BY-ND 4.0 International license.

5:1595-608.

100. Vandeputte D, Kathagen G, D'Hoe K, Vieira-Silva S, Valles-Colomer M, Sabino J, Wang J, Tito RY, De Commer L, Darzi Y, Vermeire S, Falony G, Raes J. 2017. Quantitative microbiome profiling links gut community variation to microbial load. Nature 551:507-511.

101. Ramseier CA, Kinney JS, Herr AE, Braun T, Sugai JV, Shelburne CA, Rayburn LA, Tran HM, Singh AK, Giannobile WV. 2009. Identification of pathogen and host-response markers correlated with periodontal disease. J Periodontol 80:436-46.

102. Rasmussen R. 2001. Quantification on the LightCycler, p 21-34, Rapid cycle real-time PCR. Springer.

103. Hellemans J, Mortier G, De Paepe A, Speleman F, Vandesompele J. 2007. qBase relative quantification framework and software for management and automated analysis of real-time quantitative PCR data. Genome Biol 8:R19.

104. Illumina I. 2013. 16S Metagenomic sequencing library preparation. Preparing 16S Ribosomal RNA Gene Amplicons for the Illumina MiSeq System:1-28.

105. R Core Team. 2013. R: A language and environment for statistical computing.

106. Callahan BJ, McMurdie PJ, Rosen MJ, Han AW, Johnson AJA, Holmes SP. 2016. DADA2: high-resolution sample inference from Illumina amplicon data. Nat Methods 13:581-583.

107. Bolyen E, Rideout JR, Dillon MR, Bokulich NA, Abnet CC, Al-Ghalith GA, Alexander H, Alm EJ, Arumugam M, Asnicar F, Bai Y, Bisanz JE, Bittinger K,

bioRxiv preprint doi: https://doi.org/10.1101/2020.05.08.083899; this version posted May 9, 2020. The copyright holder for this preprint (which was not certified by peer review) is the author/funder, who has granted bioRxiv a license to display the preprint in perpetuity. It is made available under aCC-BY-ND 4.0 International license.

Brejnrod A, Brislawn CJ, Brown CT, Callahan BJ, Caraballo-Rodríguez AM, Chase J, Cope EK, Da Silva R, Diener C, Dorrestein PC, Douglas GM, Durall DM, Duvallet C, Edwardson CF, Ernst M, Estaki M, Fouquier J, Gauglitz JM, Gibbons SM, Gibson DL, Gonzalez A, Gorlick K, Guo J, Hillmann B, Holmes S, Holste H, Huttenhower C, Huttley GA, Janssen S, Jarmusch AK, Jiang L, Kaehler BD, Kang KB, Keefe CR, Keim P, Kelley ST, Knights D, et al. 2019. Reproducible, interactive, scalable and extensible microbiome data science using QIIME 2. Nat Biotechnol 37:852-857.

108. Bokulich NA, Kaehler BD, Rideout JR, Dillon M, Bolyen E, Knight R, Huttley GA, Caporaso JG. 2018. Optimizing taxonomic classification of marker-gene amplicon sequences with QIIME 2's q2-feature-classifier plugin. Microbiome 6:90.

109. Quast C, Pruesse E, Yilmaz P, Gerken J, Schweer T, Yarza P, Peplies J, Glockner FO. 2013. The SILVA ribosomal RNA gene database project: improved data processing and web-based tools. Nucleic Acids Res 41:D590-6.

110. Janssen S, McDonald D, Gonzalez A, Navas-Molina JA, Jiang L, Xu ZZ, Winker K, Kado DM, Orwoll E, Manary M. 2018. Phylogenetic placement of exact amplicon sequences improves associations with clinical information. mSystems 3:e00021-18.

111. Bisanz JE. 2019. qiime2R: Importing QIIME2 artifacts and associated data into R sessions.

112. McMurdie PJ, Holmes S. 2013. phyloseq: an R package for reproducible

bioRxiv preprint doi: https://doi.org/10.1101/2020.05.08.083899; this version posted May 9, 2020. The copyright holder for this preprint (which was not certified by peer review) is the author/funder, who has granted bioRxiv a license to display the preprint in perpetuity. It is made available under aCC-BY-ND 4.0 International license.

interactive analysis and graphics of microbiome census data.

113. Lahti L, Shetty S, Blake T, Salojarvi J. 2017. Microbiome r package. Tools Microbiome Anal R.

114. Kembel SW, Cowan PD, Helmus MR, Cornwell WK, Morlon H, Ackerly DD, Blomberg SP, Webb CO. 2010. Picante: R tools for integrating phylogenies and ecology. Bioinformatics 26:1463-4.

115. Weiss S, Xu ZZ, Peddada S, Amir A, Bittinger K, Gonzalez A, Lozupone C, Zaneveld JR, Vázquez-Baeza Y, Birmingham A. 2017. Normalization and microbial differential abundance strategies depend upon data characteristics. Microbiome 5:27.

116. Martino C, Morton JT, Marotz CA, Thompson LR, Tripathi A, Knight R, Zengler K. 2019. A novel sparse compositional technique reveals microbial perturbations. mSystems 4:e00016-19.

117. Silverman JD, Washburne AD, Mukherjee S, David LA. 2017. A phylogenetic transform enhances analysis of compositional microbiota data. Elife 6:e21887.

118. Bates D, Mächler M, Bolker B, Walker S. 2015. Fitting linear mixed-effects models using lme4. J Stat Softw 67:1-48.

119. Goode K, Rey K. 2019. ggResidpanel: panels and interactive versions of diagnostic plots using 'ggplot2'.

120. Kuznetsova A, Brockhoff PB, Christensen RHB. 2017. lmerTest package: tests in linear mixed effects models. J Stat Softw 82.

121. Lenth R. 2019. emmeans: estimated marginal means, aka least-squares means.

bioRxiv preprint doi: https://doi.org/10.1101/2020.05.08.083899; this version posted May 9, 2020. The copyright holder for this preprint (which was not certified by peer review) is the author/funder, who has granted bioRxiv a license to display the preprint in perpetuity. It is made available under aCC-BY-ND 4.0 International license.

122. Anderson MJ. 2001. A new method for non-parametric multivariate analysis of variance. Austral Ecol 26:32-46.

123. Anderson MJ. 2006. Distance-based tests for homogeneity of multivariate dispersions. Biometrics 62:245-253.

124. Oksanen J, Blanchet FG, Friendly M, Kindt R, Legendre P, McGlinn D, Minchin PR, O'Hara RB, Simpson GL, Solymos P, Stevens MHH, Szoecs E, Wagner H. 2019. vegan: Community Ecology Package.

bioRxiv preprint doi: https://doi.org/10.1101/2020.05.08.083899; this version posted May 9, 2020. The copyright holder for this preprint (which was not certified by peer review) is the author/funder, who has granted bioRxiv a license to display the preprint in perpetuity. It is made available under aCC-BY-ND 4.0 International license.

Tables

Table 1. PERMANOVA results and subsequent conditional contrasts.

Distance matrix	Main effects		Interaction	Conditional contrasts			
	Diet	Sample origin		REF-DID VS. IM-DID	REF-DIM VS. IM-DIM	REF-DID VS. REF-DIM	IM-DID VS. IM-DIM
Jaccard	0.001	0.001	0.001	0.001	0.001	0.001	0.001
Unweighted UniFrac	0.001[1]	0.001	0.001	0.001[1]	0.001	0.001	0.001
Aitchison	0.001	0.003	0.004	0.002	0.004	0.004[1]	0.002[1]
PHILR (Euclidean)[2]	0.001	0.001	0.001	0.001	0.005	0.001	0.001

REF, reference diet; IM, insect meal diet; DID, distal intestine digesta; DIM, distal intestine mucosa.

[1]Monte Carlo *p* value.

[2]Phylogenetic isometric log-ratio transformed Euclidean distance.

bioRxiv preprint doi: https://doi.org/10.1101/2020.05.08.083899; this version posted May 9, 2020. The copyright holder for this preprint (which was not certified by peer review) is the author/funder, who has granted bioRxiv a license to display the preprint in perpetuity. It is made available under aCC-BY-ND 4.0 International license.

1048 **Table 2. Test of homogeneity of multivariate dispersions among groups.**

Distance matrix	Conditional contrasts			
	REF-DID VS. IM-DID	REF-DIM VS. IM-DIM	REF-DID VS. REF-DIM	IM-DID VS. IM-DIM
Jaccard	0.002	0.087	0.045	0.002
Unweighted UniFrac	0.002	0.711	0.200	0.002
Aitchison	0.453	0.046	0.046	0.369
PHILR (Euclidean)[1]	0.240	0.266	0.240	0.266

1049 REF, reference diet; IM, insect meal diet; DID, distal intestine digesta; DIM, distal intestine mucosa.

1050 [1]Phylogenetic isometric log-ratio transformed Euclidean distance.

bioRxiv preprint doi: https://doi.org/10.1101/2020.05.08.083899; this version posted May 9, 2020. The copyright holder for this preprint (which was not certified by peer review) is the author/funder, who has granted bioRxiv a license to display the preprint in perpetuity. It is made available under aCC-BY-ND 4.0 International license.

Figures

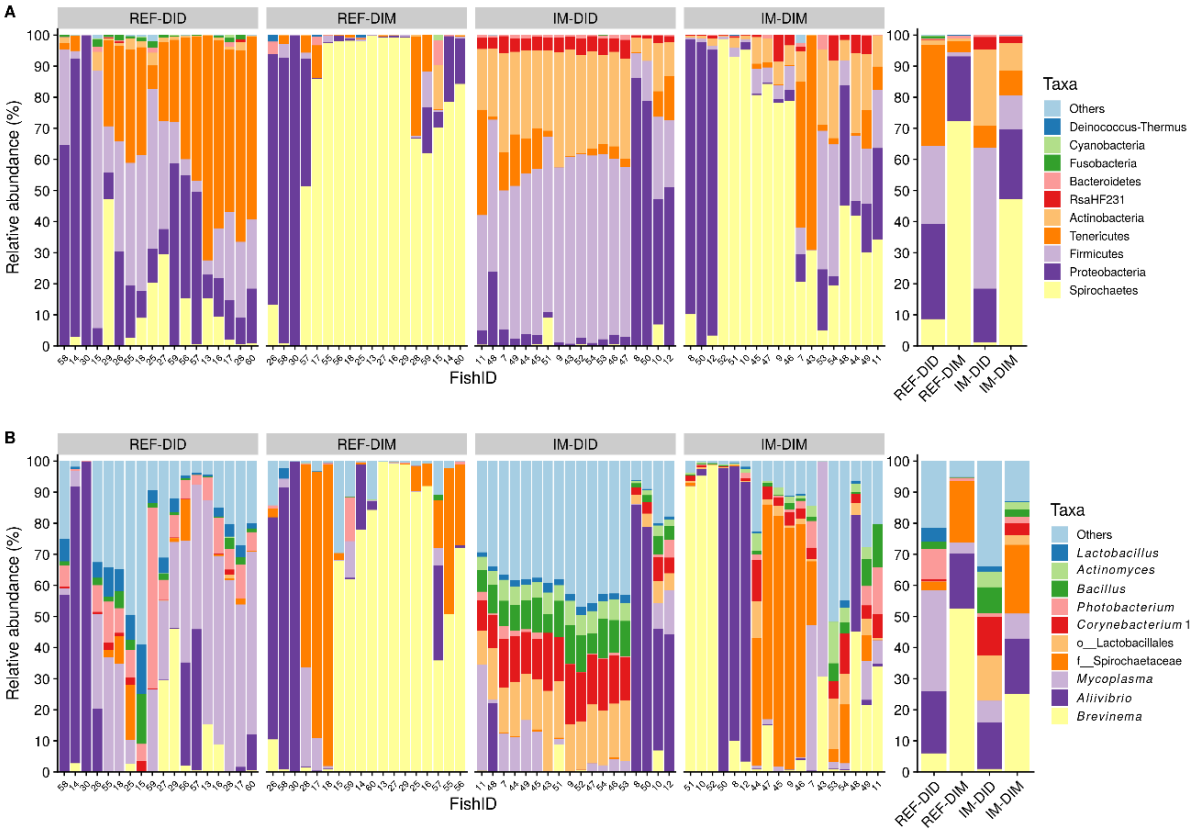

Figure 1. Top 10 most abundant taxa of all samples at phylum (A) and genus (B) level. The samples are grouped by sample origins and dietary treatments. The mean relative abundance of each taxon within the same group is displayed on the right side. o__, order; f__, family; REF, reference diet; IM, insect meal diet; DID, distal intestine digesta; DIM, distal intestine mucosa.

bioRxiv preprint doi: https://doi.org/10.1101/2020.05.08.083899; this version posted May 9, 2020. The copyright holder for this preprint (which was not certified by peer review) is the author/funder, who has granted bioRxiv a license to display the preprint in perpetuity. It is made available under aCC-BY-ND 4.0 International license.

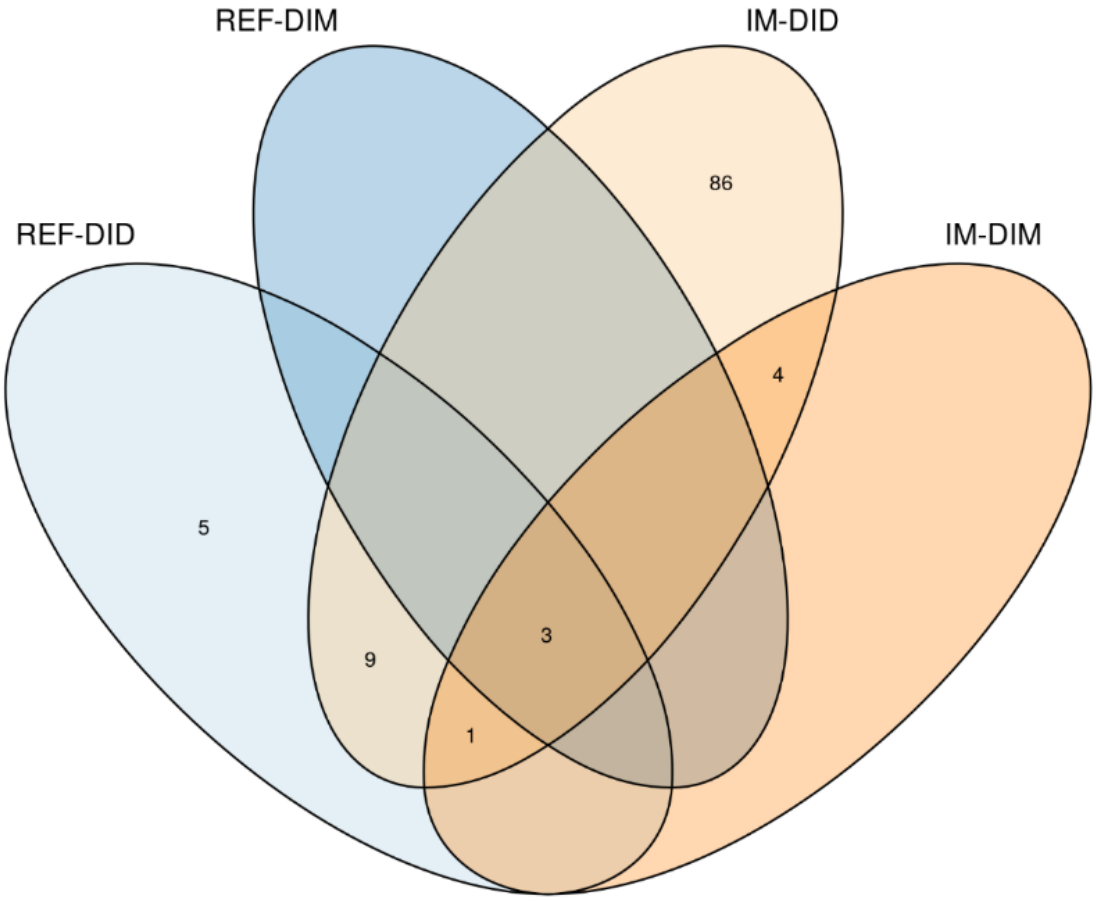

1057 **Figure 2. Venn's diagram showing the shared and unique core microbiota in each**

1058 **sample type.** The core microbiota was computed using a prevalence threshold of 80%.

1059 REF, reference diet; IM, insect meal diet; DID, distal intestine digesta; DIM, distal

1060 intestine mucosa.

bioRxiv preprint doi: https://doi.org/10.1101/2020.05.08.083899; this version posted May 9, 2020. The copyright holder for this preprint (which was not certified by peer review) is the author/funder, who has granted bioRxiv a license to display the preprint in perpetuity. It is made available under aCC-BY-ND 4.0 International license.

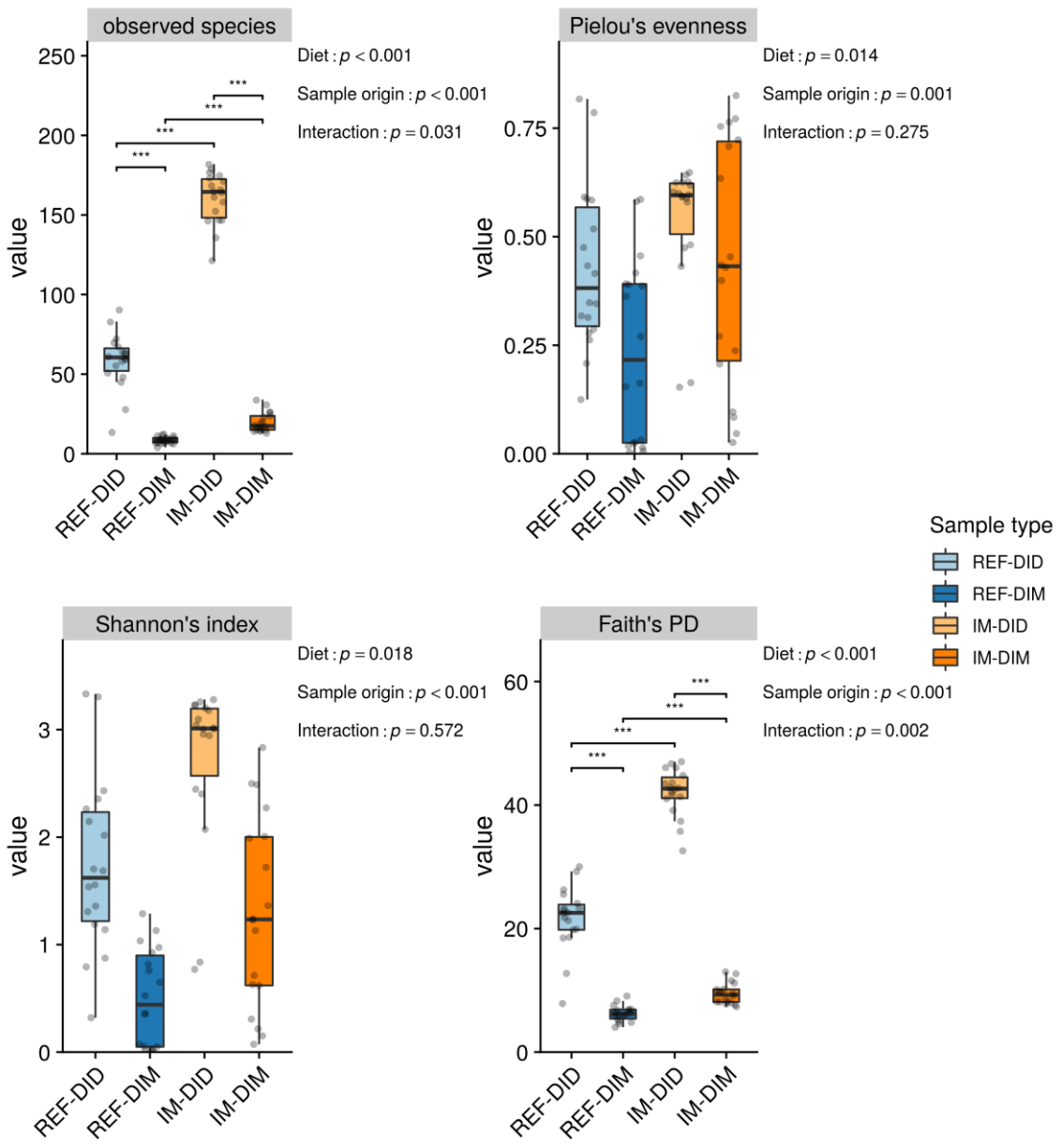

Figure 3. The sample origin and diet effects on the alpha-diversity of distal intestinal microbiota in seawater phase Atlantic salmon. The *p* value of the main effects and their interaction are displayed on the top-right corner of each sub-plot. Asterisks denote statistically significant differences (*, $p < 0.05$; **, $p < 0.01$; ***, $p < 0.001$). PD, phylogenetic diversity; REF, reference diet; IM, insect meal diet; DID, distal intestine digesta; DIM, distal intestine mucosa.

bioRxiv preprint doi: https://doi.org/10.1101/2020.05.08.083899; this version posted May 9, 2020. The copyright holder for this preprint (which was not certified by peer review) is the author/funder, who has granted bioRxiv a license to display the preprint in perpetuity. It is made available under aCC-BY-ND 4.0 International license.

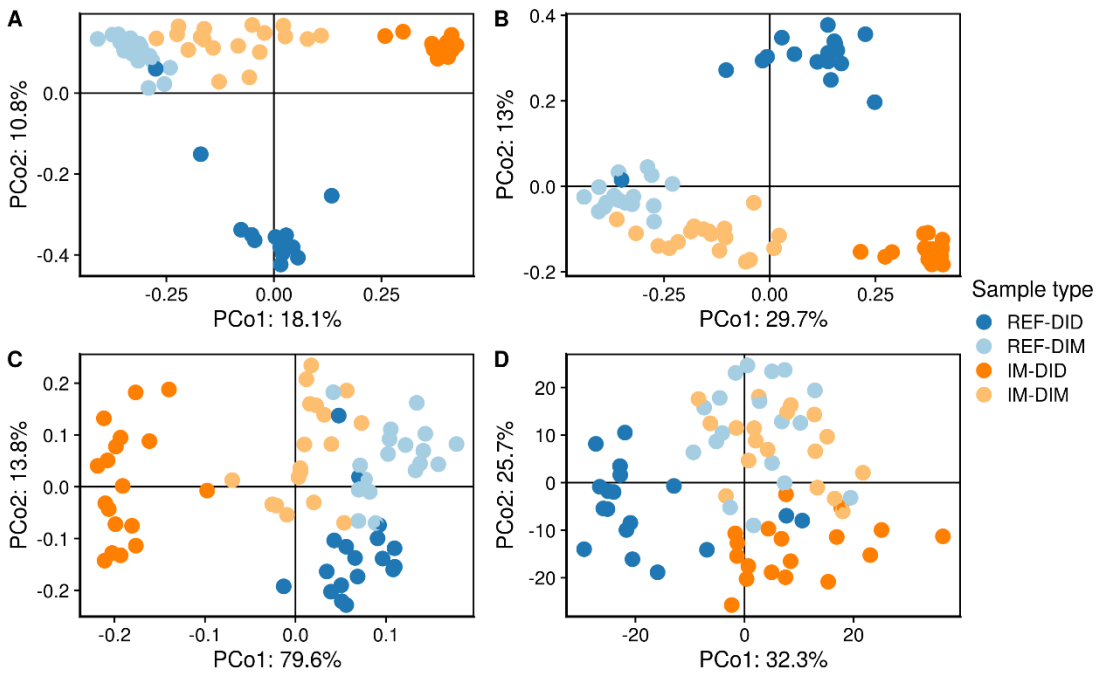

1067 **Figure 4. The sample origin and diet effects on the beta-diversity of distal intestinal**

1068 **microbiota in seawater phase Atlantic salmon.** The PCoA plots were built on Jaccard

1069 (A), unweighted UniFrac (B), Aitchison (C) and PHILR transformed Euclidean (D)

1070 distance matrix, respectively. PCo, principle coordinate; PHILR, phylogenetic isometric

1071 log-ratio; REF, reference diet; IM, insect meal diet; DID, distal intestine digesta; DIM,

1072 distal intestine mucosa.

bioRxiv preprint doi: https://doi.org/10.1101/2020.05.08.083899; this version posted May 9, 2020. The copyright holder for this preprint (which was not certified by peer review) is the author/funder, who has granted bioRxiv a license to display the preprint in perpetuity. It is made available under aCC-BY-ND 4.0 International license.

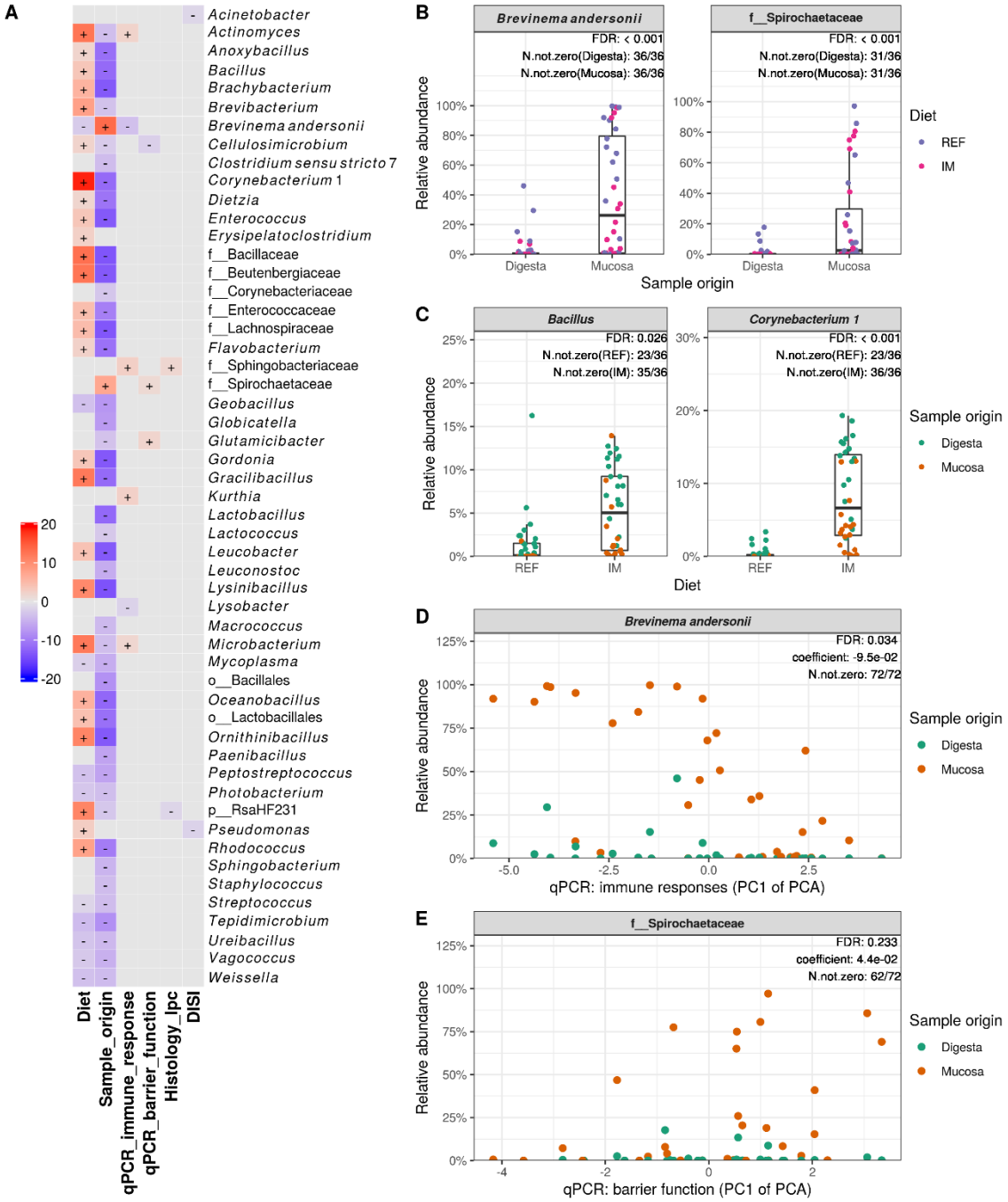

Figure 5. Significant associations between microbial clades and sample metadata. (A) Heatmap summarizing all the significant associations between microbial clades and sample metadata. Color key: -log(*q*-value) * sign(coefficient). Cells that denote significant associations are colored (red or blue) and overlaid with a plus (+) or minus (-) sign that indicates the direction of association: Diet (+), higher abundance in salmon fed the IM diet; Sample_origin (+), higher abundance in mucosa samples; Histology_lpc (+),

bioRxiv preprint doi: https://doi.org/10.1101/2020.05.08.083899; this version posted May 9, 2020. The copyright holder for this preprint (which was not certified by peer review) is the author/funder, who has granted bioRxiv a license to display the preprint in perpetuity. It is made available under aCC-BY-ND 4.0 International license.

higher abundance in salmon scored abnormal regarding lamina propria cellularity (lpc) in the distal intestine; DISI (+), positive correlation between microbial clade abundance and distal intestine somatic index (DISI); qPCR_immune_response (+) / qPCR_barrier_function (+), negative correlation between microbial clade abundance and the gene expression levels. (B) Taxa that are more abundant in the intestinal mucosa than the digesta. (C) Representative taxa showing increased relative abundances in both intestinal digesta and mucosa of salmon fed the IM diet. (D) The positive correlation between the relative abundance of *B. andersonii* and immune gene expression levels in the distal intestine. Note that the expression levels of the immune genes decreased as the PC1 of the PCA increased. (E) The negative correlation between the relative abundance of the unclassified *Spirochaetaceae* and the expression levels of barrier function relevant genes. Also note that the expression levels of the barrier function relevant genes decreased as the PC1 of the PCA increased. p__, phylum; o__, order; f__, family; FDR, false discovery rate; N.not.zero, number of observations that are not zero; REF, reference diet; IM, insect meal diet.

bioRxiv preprint doi: https://doi.org/10.1101/2020.05.08.083899; this version posted May 9, 2020. The copyright holder for this preprint (which was not certified by peer review) is the author/funder, who has granted bioRxiv a license to display the preprint in perpetuity. It is made available under aCC-BY-ND 4.0 International license.

Supplemental tables

Table S1. Contaminating features removed from the ASV table (available online).

Table S2. The prevalence of core taxa in different sample types (available online).

bioRxiv preprint doi: https://doi.org/10.1101/2020.05.08.083899; this version posted May 9, 2020. The copyright holder for this preprint (which was not certified by peer review) is the author/funder, who has granted bioRxiv a license to display the preprint in perpetuity. It is made available under aCC-BY-ND 4.0 International license.

Supplemental figures

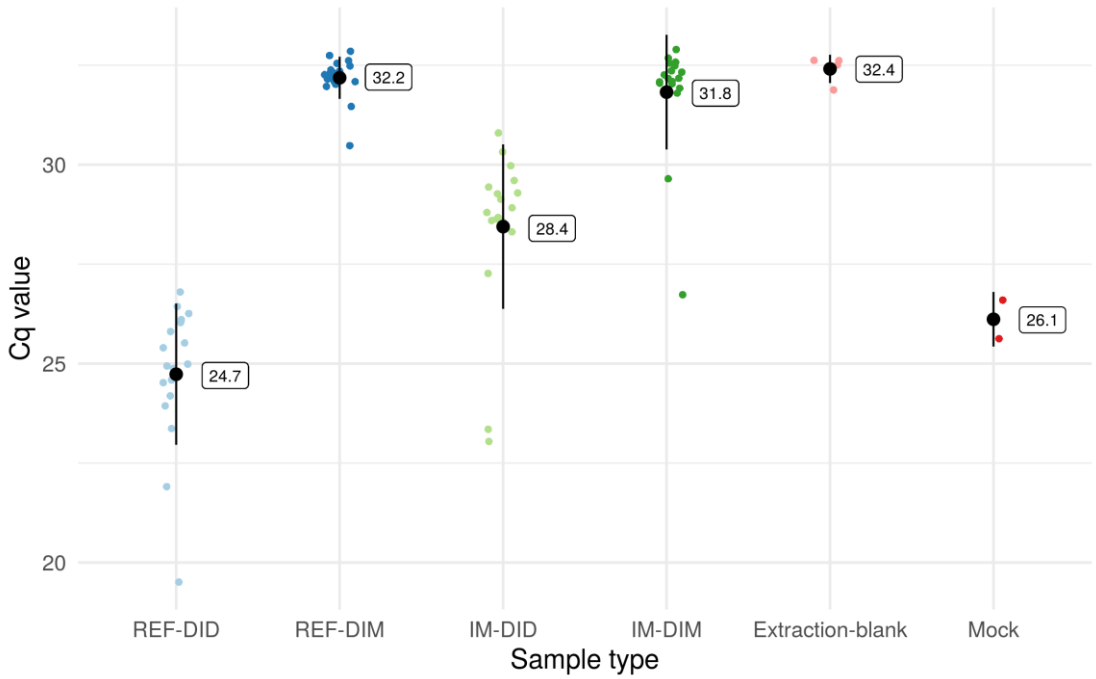

Figure S1. Quantification of bacterial 16S rRNA gene in different sample types using qPCR. Since the Cq values of most mucosa-associated samples were out of the linear range of the standard curve, the Cq value was used as a proxy of 16S rRNA gene quantity which is reliable for the screening of contaminant sequences. Data are presented as mean ± 1 standard deviation overlaying the raw data points. Abbreviations: REF, reference diet; IM, insect meal diet; DID, distal intestine digesta; DIM, distal intestine mucosa.

bioRxiv preprint doi: https://doi.org/10.1101/2020.05.08.083899; this version posted May 9, 2020. The copyright holder for this preprint (which was not certified by peer review) is the author/funder, who has granted bioRxiv a license to display the preprint in perpetuity. It is made available under aCC-BY-ND 4.0 International license.

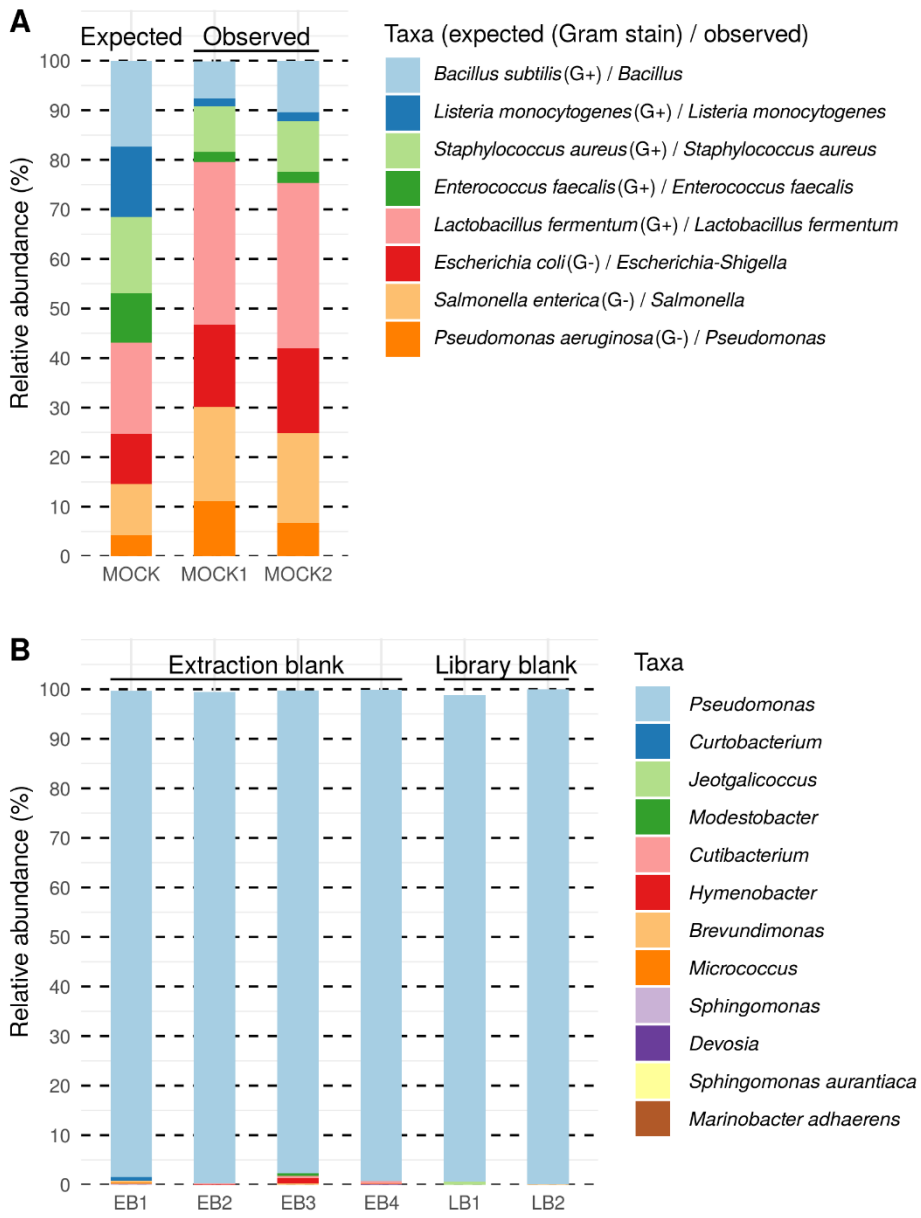

Figure S2. Taxonomic profile of the mock (A) and contaminating features in the negative controls (B). The lowest level of taxonomic ranks was displayed for each taxon. EB, extraction blank; LB, library blank.

bioRxiv preprint doi: https://doi.org/10.1101/2020.05.08.083899; this version posted May 9, 2020. The copyright holder for this preprint (which was not certified by peer review) is the author/funder, who has granted bioRxiv a license to display the preprint in perpetuity. It is made available under aCC-BY-ND-4.0 International license.

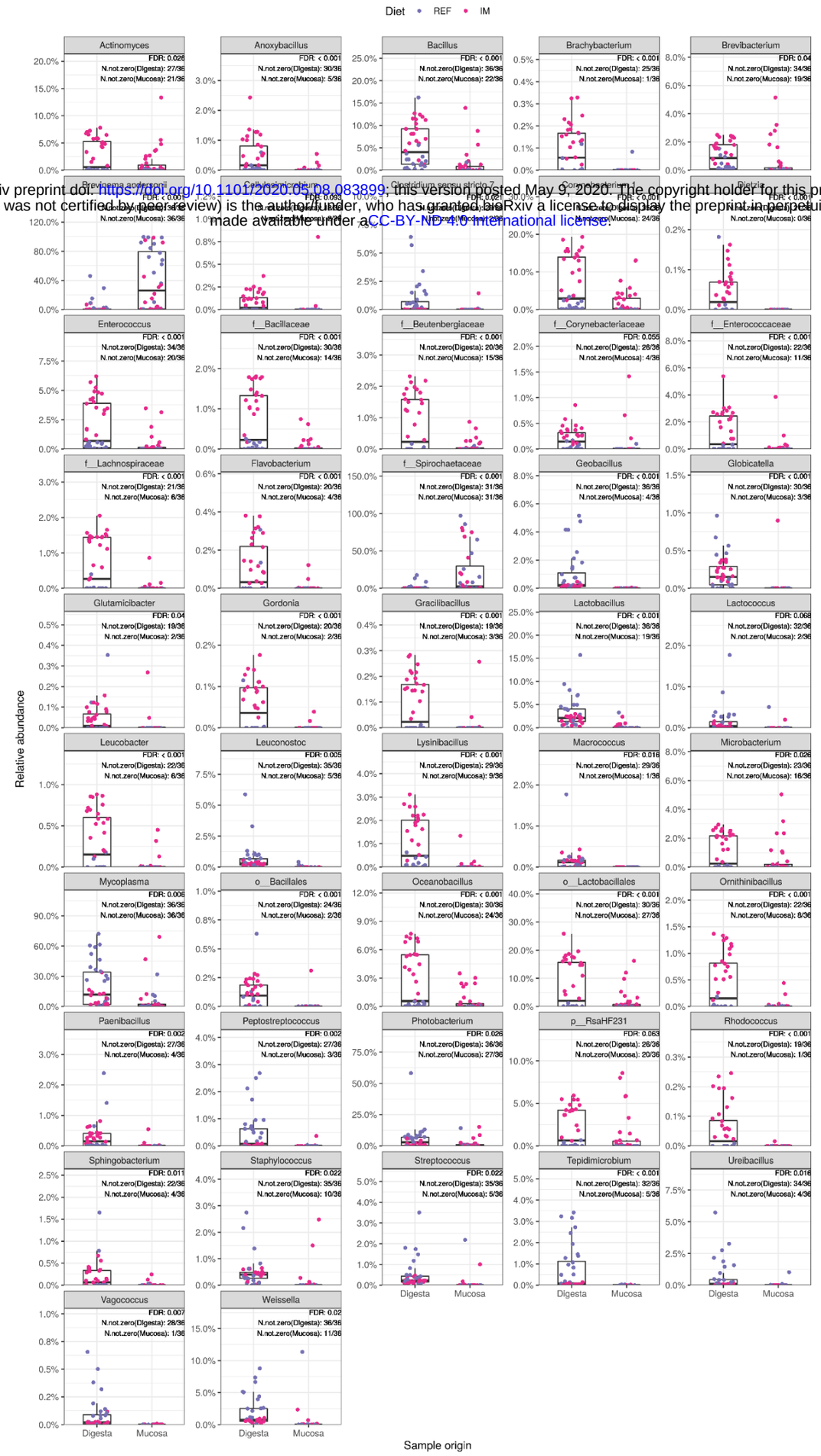

1107 **Figure S3. Microbial clades showing significant associations with sample origin.**

1108 FDR, false discovery rate; N.not.zero, number of non-zero observations; REF, reference

1109 diet; IM, insect meal diet.

bioRxiv preprint doi: https://doi.org/10.1101/2020.05.08.083899; this version posted May 9, 2020. The copyright holder for this preprint (which was not certified by peer review) is the author/funder, who has granted bioRxiv a license to display the preprint in perpetuity. It is made available under aCC-BY-ND 4.0 International license.

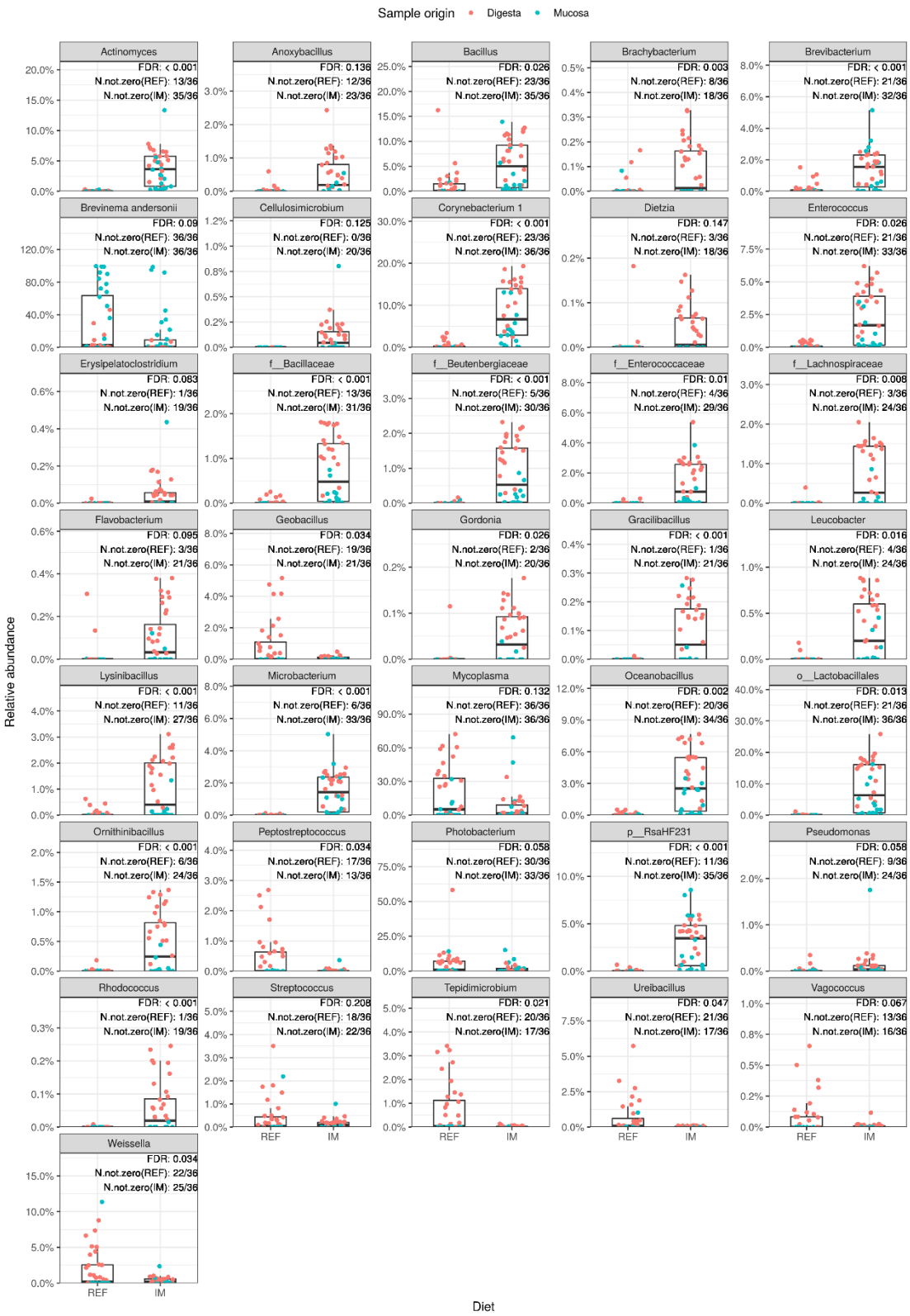

Figure S4. Microbial clades showing significant associations with diet. FDR, false discovery rate; N.not.zero, number of non-zero observations; REF, reference diet; IM, insect meal diet.

bioRxiv preprint doi: https://doi.org/10.1101/2020.05.08.083899; this version posted May 9, 2020. The copyright holder for this preprint (which was not certified by peer review) is the author/funder, who has granted bioRxiv a license to display the preprint in perpetuity. It is made available under aCC-BY-ND 4.0 International license.

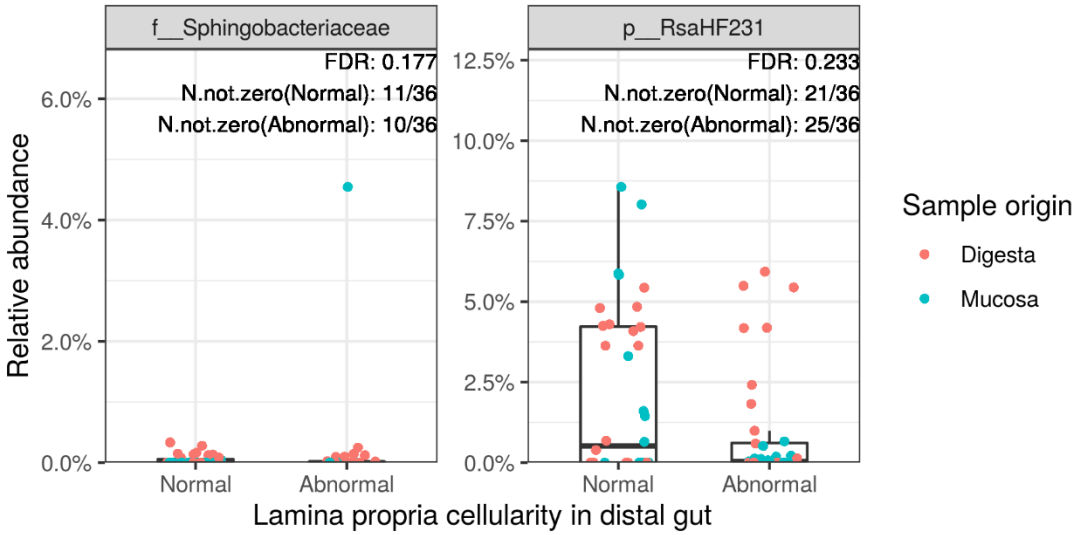

Figure S5. Microbial clades showing significant associations with histological scores on lamina propria cellularity in the distal intestine. FDR, false discovery rate; N.not.zero, number of non-zero observations.

bioRxiv preprint doi: https://doi.org/10.1101/2020.05.08.083899; this version posted May 9, 2020. The copyright holder for this preprint (which was not certified by peer review) is the author/funder, who has granted bioRxiv a license to display the preprint in perpetuity. It is made available under aCC-BY-ND 4.0 International license.

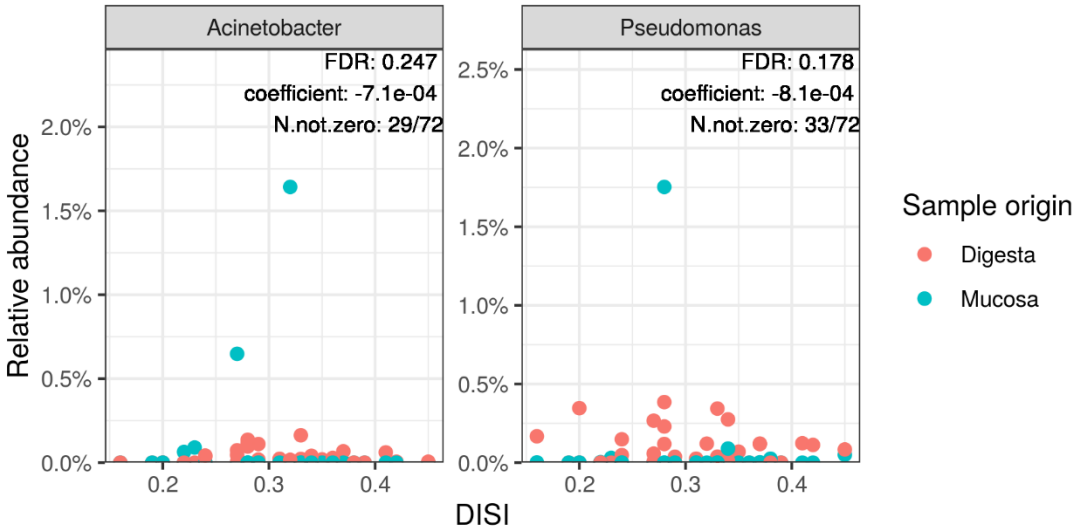

1116 **Figure S6. Microbial clades showing significant associations with distal intestine**

1117 **somatic index (DISI).** FDR, false discovery rate; N.not.zero, number of non-zero

1118 observations.

bioRxiv preprint doi: https://doi.org/10.1101/2020.05.08.083899; this version posted May 9, 2020. The copyright holder for this preprint (which was not certified by peer review) is the author/funder, who has granted bioRxiv a license to display the preprint in perpetuity. It is made available under aCC-BY-ND 4.0 International license.

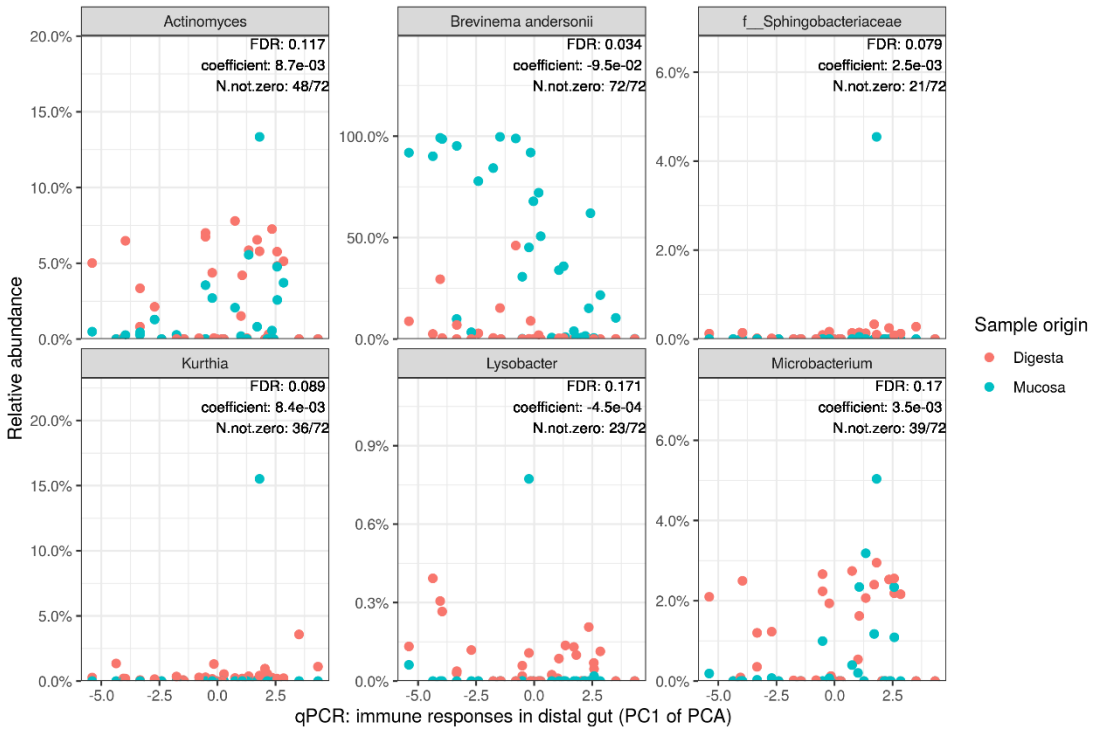

Figure S7. Microbial clades showing significant associations with immune gene expressions in the distal intestine. Since the expression levels of immune genes were highly correlated, we ran a principle component analysis (PCA) and used the first principle component (PC1) for the association testing to avoid multicollinearity and reduce the number of association testing. Note that the expression levels of immune genes decrease as the PC1 increases from left to right. Hence, a positive correlation coefficient denotes a negative association between the microbial clade and immune gene expressions, and vice versa. FDR, false discovery rate; N.not.zero, number of non-zero observations.

bioRxiv preprint doi: https://doi.org/10.1101/2020.05.08.083899; this version posted May 9, 2020. The copyright holder for this preprint (which was not certified by peer review) is the author/funder, who has granted bioRxiv a license to display the preprint in perpetuity. It is made available under aCC-BY-ND 4.0 International license.

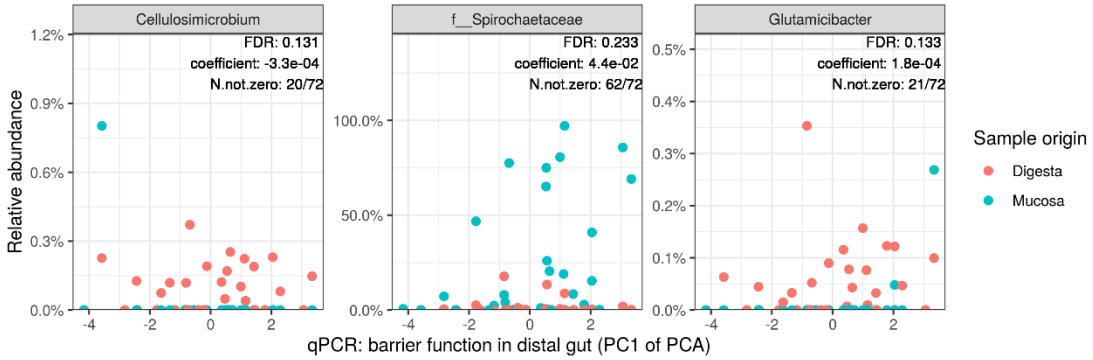

Figure S8. Microbial clades showing significant associations with expressions of barrier function related genes in the distal intestine. Since the expression levels of barrier function related genes were highly correlated, we ran a principle component analysis (PCA) and used the first principle component (PC1) for the association testing to avoid multicollinearity and reduce the number of association testing. Note that the expression levels of barrier function related genes decrease as the PC1 increases from left to right. Hence, a positive correlation coefficient denotes a negative association between the microbial clade and barrier function related gene expressions, and vice versa. FDR, false discovery rate; N.not.zero, number of non-zero observations.